Adhesion Theory for Low Friction on Ice

Katsutoshi Tusima
University of Toyama
Japan

1. Introduction

Ice is one of the lowest frictional materials on the earth. Its low friction enables us to utilize for enjoyment of skating, skiing and sledging.

Why friction on ice is so low? It has been known since ancient times that a liquid lubricant such as oil can reduce the friction, and many scientists have analogically guessed that water formed at the interface between ice and a slider may serve as lubricant. Two theories have been proposed to explain the formation of liquid water at the interface: one relates it to pressure melting (Joly, 1887; Reynolds, 1899) and other to friction melting (Bowden & Hughes, 1939). Bowden and Hughes obtained for μ_k between the plates and rotating ice disk a large value of 0.3 at a velocity of 30 mm/s against a small value of 0.04 at a higher velocity of 5 m/s. This experimental result has been essential basis in friction melting theory.

Pressure melting theory has been abandoned because heat must be carried from temperature region higher than real contact area. Friction melting theory has been supported by Bowden (1953, 1955), Shimbo (1961), Barnes et al. (1979), Evans et al. (1976) and other many reseacher to explain their experiments. Also, Huzioka (1962, 1963) observed the refreezed icicles appeared snow grains and Tusima & Yosida (1969) observed the splashed water from interface between a rotating disk of ice and an annular slider at high-speed friction (10~20m/s). Hence, the existence of liquid water has been generally accepted as the cause of the low frictional coefficient of ice. Other speculative theories have been proposed by Weyl (liquid-like layer, 1951), Niven (rotation of ice molecules, 1959), McConica (vapor lubrication, 1959), Huzioka (sintering, 1962), and Tusima (adhesion theory, 1976, 1977).

The frictional melting theory thought that the melted water prevented the direct contact of two surfaces and lubricated between slider and ice as self-lubrication. This speculation introduced by similarity that small coefficient of friction may be inherent to liquid lubrication without examination feasibility of adhesion theory. So that, in many cases, it has been missed the following important property concerning to the friction process of ice: hardness and shear strength of ice, adhesive strength, real contact area, observation of frictional track, qualitative explanation of frictional resistance, etc. Several contradictory report have been presented on μ_k of ice in the absence of liquid water. Tabor & Walker (1970) and Barnes et al. (1971) obtained a low value of 0.05 for μ_k between an ice cone and a stainless steel plane in a velocity from 10^{-5} to 10^2 mm/s. Tusima (1977) obtained 0.005 to 0.1 for μ_k in low velocity range 0.1mm/s. Even if liquid lubrication were exist, we don't know reliable thickness of melt water for lubrication, because one scientist say few μm (Bowden &

Hughes, 1939; Ambach & Mayr, 1981) and other say few nm as thickness of melted water (Evans et al., 1976). However, frictional anisotropy changed unavailable the liquid lubrication. This anisotropy of ice can explain only by adhesion theory.

We can point out logical question for liquid lubrication theory that the water must be melted by frictional heat. Namely, if the friction was too small for production melt-water, the friction should be large in view of the theory. This is clear logical contradiction. Huzioka (1962) indicated high friction coefficient of 0.3 when remarkable icicles were observed around real contact area of snow grains. In speed skating, μ_k is extremely small, nearly 0.005 (Kobayashi, 1973; Koning et al., 1992; Tusima et al., 2000). Under these extremely low friction, skate will slide without lubrication liquid. Therefore (0001) ice rinks could display the properties of crystallographic plane of ice and μ_k became smaller than normal rink. It is clear that low value 0.01 to 0.05 does not mean always the liquid water lubrication. If liquid lubrication appear, μ_k should be the value lower than 0.0001 as pointed out by Evans et al. (1976).

According to classical adhesion theory of friction, frictional coefficient μ_k is given by

$$\mu_k = s/p + (\text{ploughing and other term})$$

where s is adhesive shear strength of real contact, roughly equal to bulk shear strength of weaker material, p is the pressure of real contact area, nearly equal to the Brinnel hardness of softer material. Ice has extremely small shear strength s (1MPa at -10°C) compared to hardness (100MPa at -10°C). Therefore, μ_k becomes nearly 0.01 under dry friction. This means ice has an inherent low friction materia. In generally, second term is too small and can neglect (however in ice, this term can not always neglect depend on shape of slider.)

The narrow water between ice and material can not apply bulk contact angle and behave abnormal as shown by Hori (1956) and Jellinek (1967). Itagaki & Huber (1989) noticed that the effect of squeeze out will thin water layer in real contact area as shown by Furushima (1972).

2. Physical properties of ice

2.1 Hardness of ice

Fiction occurs at real contact area. When hard steel ball slides on flat plate of ice, real contact area will be formed by the plastic deformation of ice. The pressure of real contact decrease in
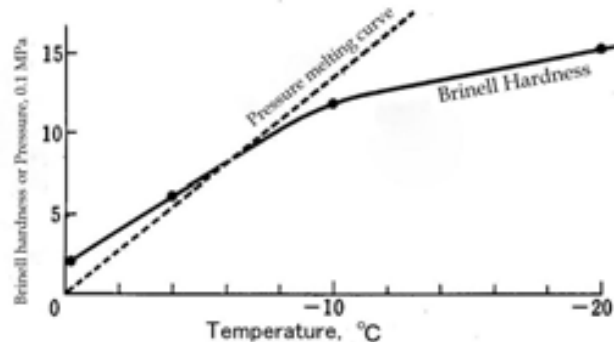

Fig. 1. Brinell hardness of single crystal of ice (Mendenhall Glacier ice) (from Butkovich, 1954), solid line and for polycrystalline of ice (from Barnes & Tabor,1966), dashed line shows pressure melting curve.

the process of plastic deformation, it will attain area depend on the sliding condition. However it is difficult to estimate an exact area in the sliding process on ice. When hard steel ball slides on flat plate of ice, apparent contact area is only one, the area will be equal to real area. The area will be given by the Brinell hardness. Butkovich (1954) measured the Brinell hardness as a function of temperature and loading time, by the use of indenter diameter 3.2mm. The result shows in Fig. 1 and Table 1. Hardness changed by crystallographic plane of ice (parallel and perpendicular to c-axis), temperature and loading time. The value increased with lowering temperature.

Temperature °C	Butkovich[1]		Barnes & Tabor[2] polycrystalline	Bowden & Tabor[3] polycrystalline
	∥ C-axis	⊥C-axis		
-0.25				18
-2			30	
-4	60	77		
-5			45	34
-10	118		60	
-15	125	111		
-20	145	126	90	60

[1] Indenter 1/8"ball, single crystal of Mendenhall glacier, ∥ C-axis 15.4N load, ⊥ C-axis 25.2N load
[2,3] Indenter Diameter 50mm, load 1000N 2)Barnes & Tabor (1966) 3)Bowden & Tabor(1964)

Table 1. Brinell hardness of ice, p MPa(=10kgf/cm²), loading time 1 sec.

Barnes et al. also measured the Brinell hardness of ice under the load of 1000N, diameter of indenter 50mm. The value of hardness becomes lower in larger indenter than smaller one.

2.2 Shear strength of ice

If the bond of real contact area is strong enough, the break will occur in inside of ice in sliding process. In generally, the value will not exceed the shear strength of ice itself. Therefore it is interested in shear strength of ice.

Temperature °C	Jellinek MPa	Raraty & Tabor MPa	Butkovich MPa	Tusima & Fujii(1973)	
				∥ C-axis	⊥C-axis
-2	0.2			1.8	2.7
-5	0.5	0.8	1.37		
-10	1.2	1.6	1.55	2.2	3.3
-15	1.5				
-20		3.1		2.6	4.3
-30		5.1	2.17	2.9	5.5

Table 2. Shear strength of ice, S MPa

Table 2 shows the measured value in several experiments. The value was very low 0.5~1.4 MPa at -5°C, and 1.2~3.3 MPa at -10°C in comparison to hardness of same temperature. The ratio s/p gives μ_k of ice in adhesion theory. From table 1 and 2, μ_k is estimated about 0.007~0.09 at -5°C and 0.01~0.07 at -10°C.

2.3 Adhesive strength of ice

There are many studies on adhesive strength of ice to other materials. Some results are shown in Table 3. It is noticed that the value of table is 1 order smaller than bulk shear strength of ice (Table 2).

Brunner (1952) MPa	Landy & Freiberger (1967) -12°C, MPa	Jellinek (1970) -4.5°C, MPa
metal 0.95 polystyrene 0.59 paraffin 0.46	PTFE 0.32 PE 0.26 PMMA 0.64	stainless rough 0.61 polish 0.3 mirror 0.06

Table 3. Adhesive shear strength of ice

Jellinek (1970) showed the effect of surface roughness of stainless steel as shown in each surfaces noticeably cleaned. We know that the adhesive strength is smaller than shear strength of ice in experience.

3. Friction of steel ball on single crystal of ice

The sliding of hard spherical surface on flat plate has been used for fundamental study of the mechanism of friction between materials (Bowden & Tabor, 1950). In this sliding, apparent contact area will be equal to real contact area. Therefore it gives to possibility qualitative evaluation for friction.

3.1 Experimental apparatus

The apparatus is shown schematically in Fig. 2. A rectangular-shaped ice sample was onto PMMA (Polymethylmethacrylate) disk A, which was mounted on a metal block M. The block M was driven either forwards or backwards on the upper surface of the thick rigid framework by a motor through reduction worm gears, and the ice sample on it was moved at a constant speed ranging from 1.5×10^{-7} to 7.4×10^{-3} m/s. Apparatus adjusted to 1mm/m by precise level.

A steel ball, 6.4 mm in diameter, contacting the ice surface was mounted and fixed to a brass cylinder, to the top of which a metal lever L was firmly fixed. One end of the lever was free, while the other end was connected to a universal joint. A load which ranged from 0.4 to 31 N, was exerted onto the ice surface by suspending a weight the lever. The weight which corresponds to a given load was immersed in an oil bath that prevented the weight from shaking.

The friction force between the fixed steel ball the moving ice surface was continuously measured by the use of a force-measuring system which consisted of transducer, a bridge box, a strain meter and recorder. The ice sample can be shifted in the transverse direction by moving the mount M so that each friction run may be made on a virgin ice surface. The ice sample can also be rotated into any horizontal orientation by turning the disk A so as to measure the friction force on ice for various crystallographic orientations.

3.2 Ice samples and steel ball

Tyndall figures were artificially produced at a corner of a large single crystal of ice collected from the Mendenhall Glacier, Alaska. By the aid of the Tyndall figures, two rectangular ice pieces were simultaneously cut out from the ice crystal in a way in which the frictional surface of the one was set parallel to the crystallographic basal plane (0001) and that of the
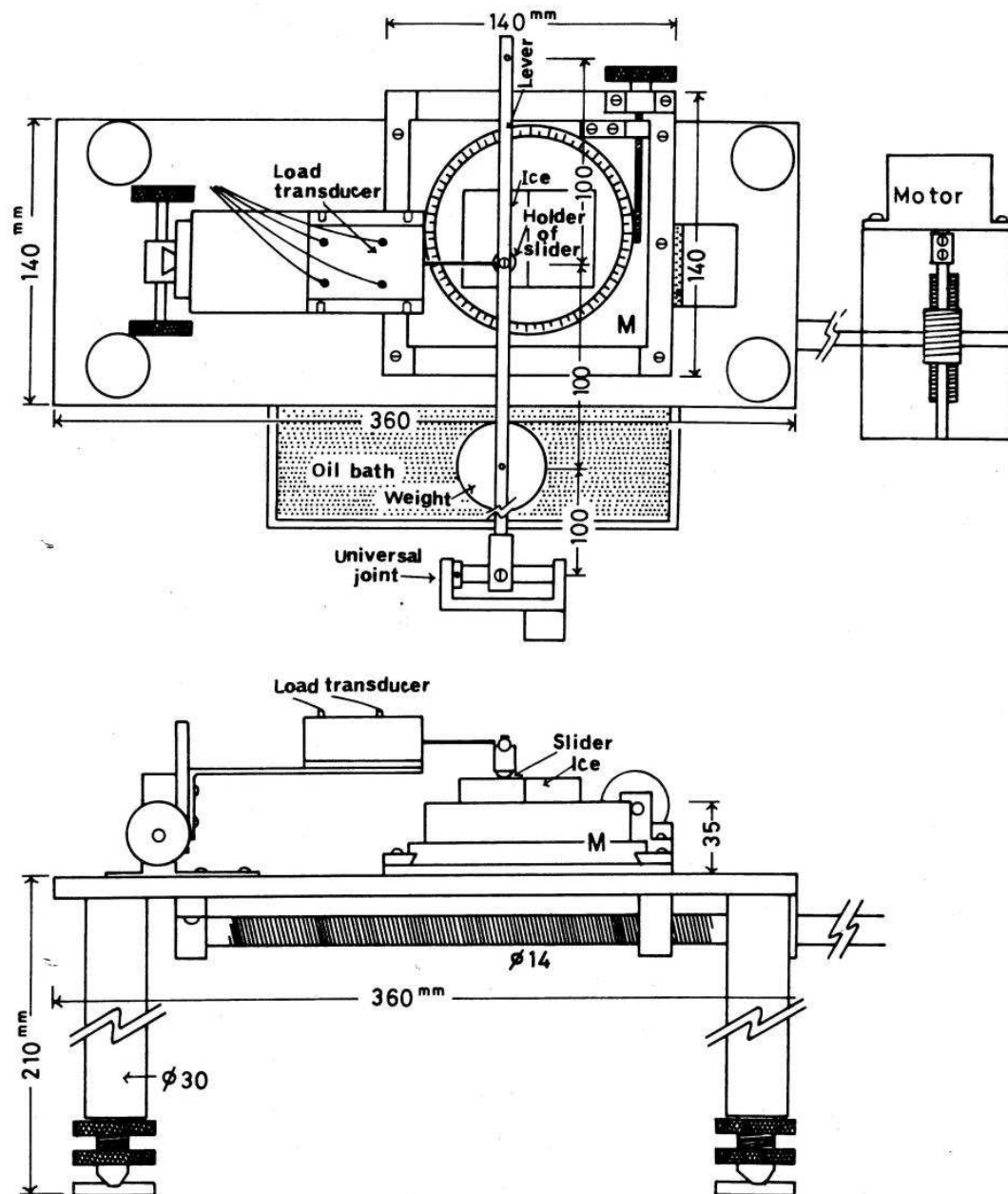
Fig. 2. Schematic diagram of the experimental apparatus.

other parallel to the prismatic plane (10$\bar{1}$0). These two pieces were placed side by side and frozen to an PMMA disk so as to form a bicrystal sample of ice. This sample was finished by lathe. It was annealed again at -3°C until the turned surface become glossy like a mirror, and then brought into a cold room at an experimental temperature of -0.5 to -30°C. When it was exposed to lower temperature than -10°C, its surface occasionally became cloudy. Such samples were excluded from the experiment, and only glossy surfaces were used experimental studies on friction.

Steel ball with different sizes ranging from 1.6 to 12.7 mm in diameter were used in the experiment. The steel ball was cleaned by immersing it in an ultrasonic cleaning-bath filled with a mixture of alcohol and acetone and then in bath filled with distilled water. The ball was cleaned again by washing it in the bath of distilled water and dried under a heating lamp.
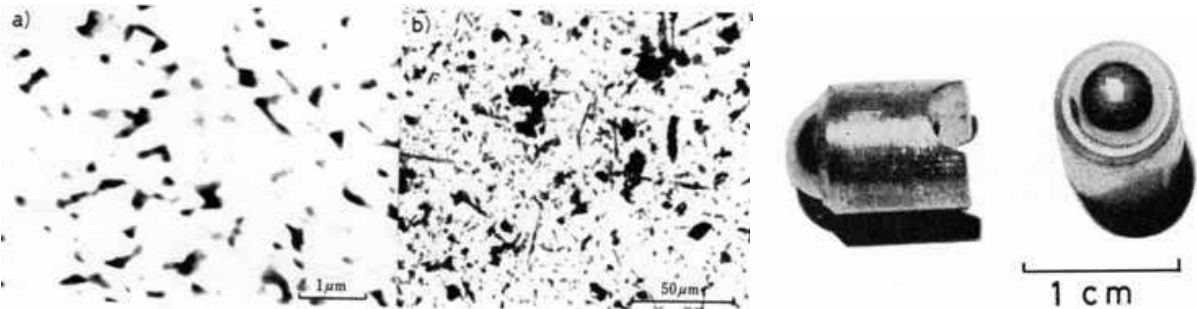
Fig. 3. A steel ball slider mounted on a brass cylinder.Left: Microscopic asperities of a slider 6.4 mm in diameter (a) tungsten carbide ball, (b)steel ball

4. Experimental results

4.1 Anisotropy of friction on crystallographic plane of ice
4.1.1 Friction curve

Steel was slid on flat plate of ice linearly connected 5 single crystal of grains as illustrated in Fig. 4. Velocity was slow as 7.4×10^{-5} m/s, temperature at -10°C, slider diameter 6.4mm of steel ball. In this condition, melting of ice does not occur. It was observed that the frictional coefficient changed by each grain. However it is noticed that the values were low as from 0.02 to 0.04.
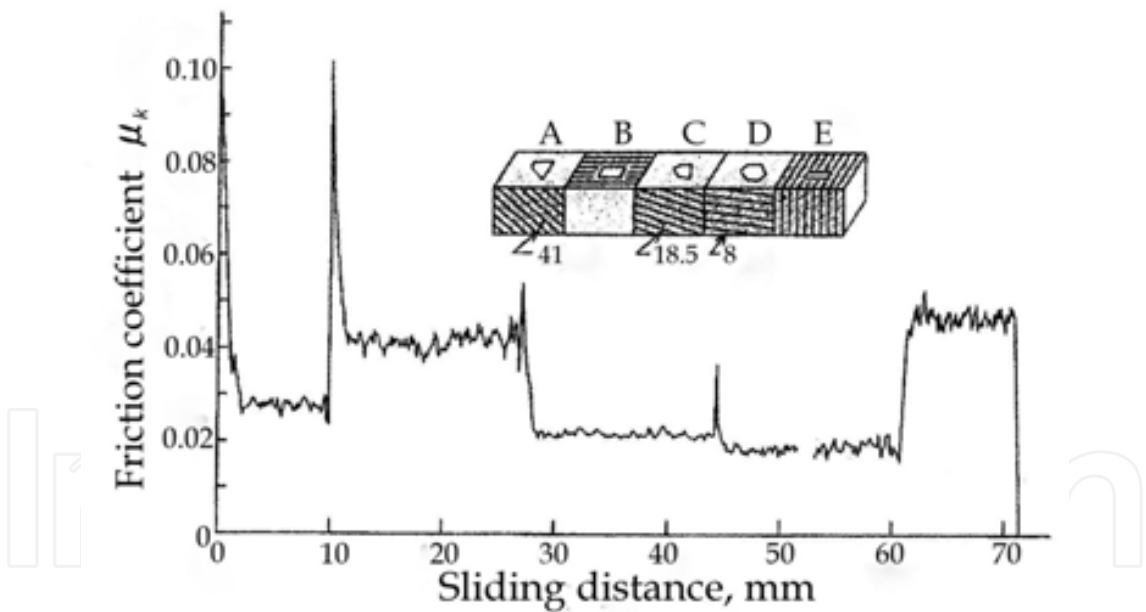

Fig. 4. Anisotropy of friction on crystallographic plane A, B, C, D, and E of ice. Longitudinal axis friction coefficient, horizontal axis sliding distance mm. Inclined lines show (0001) plane of ice. Temperature -10°C, Velocity 7.4×10^{-5} m/s, Slider diameter 6.4 mm, Load 4.7N. Inclined line shows (0001) of ice.

Anisotropy in Fig. 4 will not explain by frictional melting theory. This supports adhesion theory because the hardness, shear strength and plowing strength depend on crystallographic plane of ice. Plane (0001) of ice is most hard for vertical load and most weak for shear force because (0001) correspond to crystallographic sliding plane of ice.
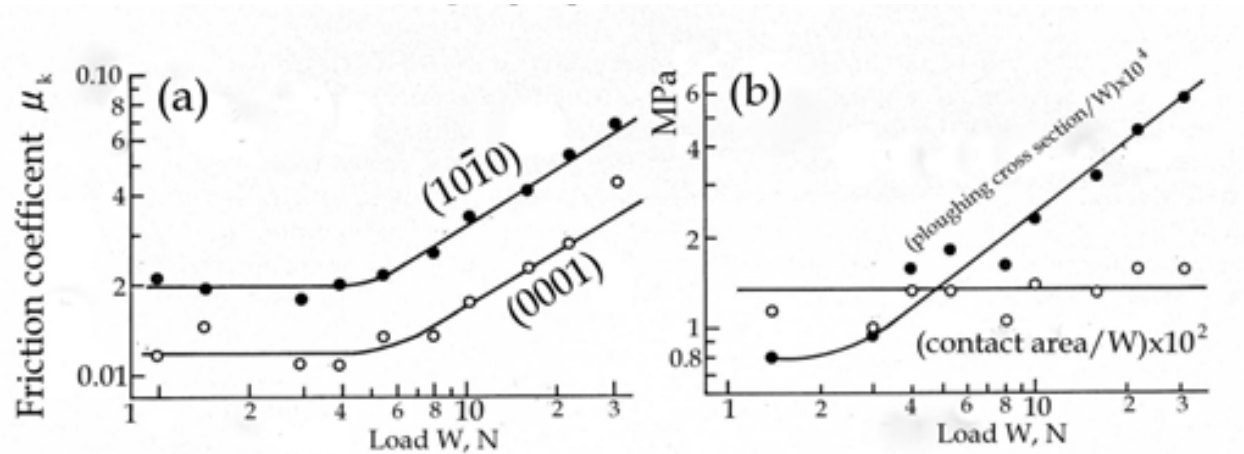
Fig. 5. (a) Dependence of friction on load for a basal and a prismatic plane of ice. (b) Contact area and ploughing cross-section against load. Velocity 7.4×10^{-5} m/s, Temperature -10°C, slider diameter 6.4 mm. ○ (0001), ● ($10\bar{1}0$) (from Tusima, 1977).

4.1.2 Load effect

As an example, μ_k for both the basal and prismatic planes, at a velocity of 7.4×10^{-5} m/s and at a temperature of -10°C, was plotted against the lower range of loads, less than 5 N for both cases, while it linearly increased with the increase in load in the higher range of load. A similar tendency to that in Fig. 5 was observed for different sliding velocities as seen in Fig. 9. The friction F in the present experiment is composed of two factors:

$$F = F_s + F_p, \tag{1}$$

where F_s and F_p respectively are concerned with the adhesion of ice and the ploughing of ice.

F_s and F_p are, respectively, proportional to A/W and A*/W, in which W is the load applied, and A and A* are the contact area and the ploughed area, respectively. It was found in the experiment that the ratio A/W is constant for any load, but the ratio A*/W increases with increasing load as shown in Fig. 5(b). Since the ploughing area A* was so small in the lower range of load, the ploughing effect was very small as compared with the sliding effect. It may, therefore, be concluded that the increase of μ_k in the higher range of load may be attributed to the increase of the ploughing effect.

As described before, it is important to measure the width of the sliding track left on the ice for interpreting the experimental results. The track width, the contact area, the average pressure acting on the contact area, and the cross-section ploughed for different loads are summarized in Table 4.

The contact area A can be expressed by using the track width φ as follows;

$$A = \pi(\varphi/2)^2 k \tag{2}$$

where k is a factor which is dependent on the visco-elastic properties of the contact area, the value of k being between 0.5 and 1.0. Fig. 6 shows the real contact area in the process of friction of a glass ball on ice. We know that the value of k is equal to 0.8 from this Fig. 6.

Load W N	Coefficient of friction μ_k	Track width, φ 10^{-3}m	Contact area, A 10^{-6} m^2	Mean pressure MPa	Ploughing area, A* 10^{-8}m^2	Calculated values		
						μ_s	μ_p	$\dfrac{\mu_s + \mu_p}{\mu_k}$
1.4	0.020	0.16	0.016	9.0	0.011	0.008	0.008	0.8
3.0	0.018	0.22	0.030	97	0.028	0.007	0.009	0.9
4.0	0.021	0.29	0.053	75	0.064	0.009	0.016	1.2
5.5	0.022	0.34	0.073	75	0.10	0.009	0.018	1.2
8.0	0.026	0.37	0.085	92	0.13	0.007	0.016	0.9
10.0	0.036	0.47	0.14	75	0.27	0.009	0.026	1.0
16.0	0.043	0.58	0.21	76	0.51	0.009	0.032	1.0
22.0	0.057	0.75	0.35	62	1.10	0.011	0.058	1.1
31.0	0.070	0.88	0.49	64	1.80	0.011	0.058	1.0

T=-10^{0}C, V=7.4×10^{-5} m/s. glacier ice ($10\bar{1}0$), S=0.7 MPa, *K*=0.8

Table 4. Some experimental results obtained in the experiment on friction of ice and the predicted values of the shear friction μ_s and the ploughing friction μ_p. (after Tusima, 1977)
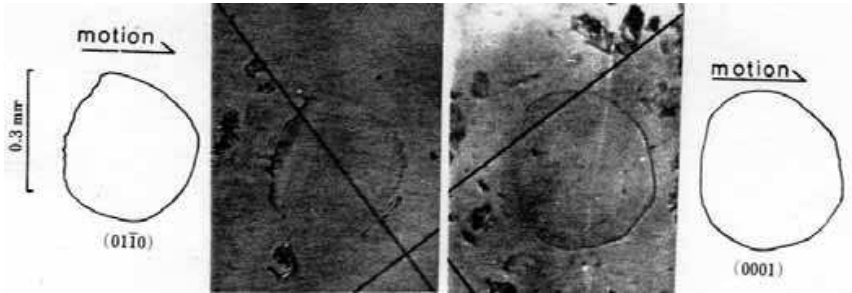

Fig. 6. Real contact area in the process of friction. Sliding of a hemispherical glass slider on a flat plate of ice coated with silicon oil to avoid condensation on the slider. Velocity: 7.4x10^{-2}mm/s, load: 4.75N left ($10\bar{1}0$), at right (0001)

4.1.3 Velocity dependence of friction

In order to clarify the dependence of the friction of ice to velocity, the friction force was measured with velocities for various loads. A typical results obtained is shown in Fig. 7, in which μ_k is plotted against the velocity obtained for both the basal and prismatic planes. As seen in this Figure, μ_k decreases with an increase in the velocity V. The width f of the track of the ball was also measured for each run of the experiment, and a similar tendency was obtained between φ and V to that obtained between μ_k and V. This shows that the larger friction at lower velocities can be attributed to the larger plastic deformation of ice at the contact area.

4.1.4 Temperature dependence of friction

The coefficient μ_k and the width of the sliding track φ are plotted in Fig. 8(a) and (b) against the ice temperature in raising process from -20°C up to -1°C at a rate of 1.5 deg/h. It was found that friction reaches a minimum at a temperature of -7°C when the sliding velocity is 7.4×10^{-5} m/s and the load is 4.8 N. As seen in this figure, the friction at a temperature below minimum friction increases on lowering the temperature, which is due to the increase of shearing strength of ice (Butkovich, 1954; Tusima & Fujii, 1973). The friction at higher temperatures above the temperature of minimum friction markedly increases as the ice
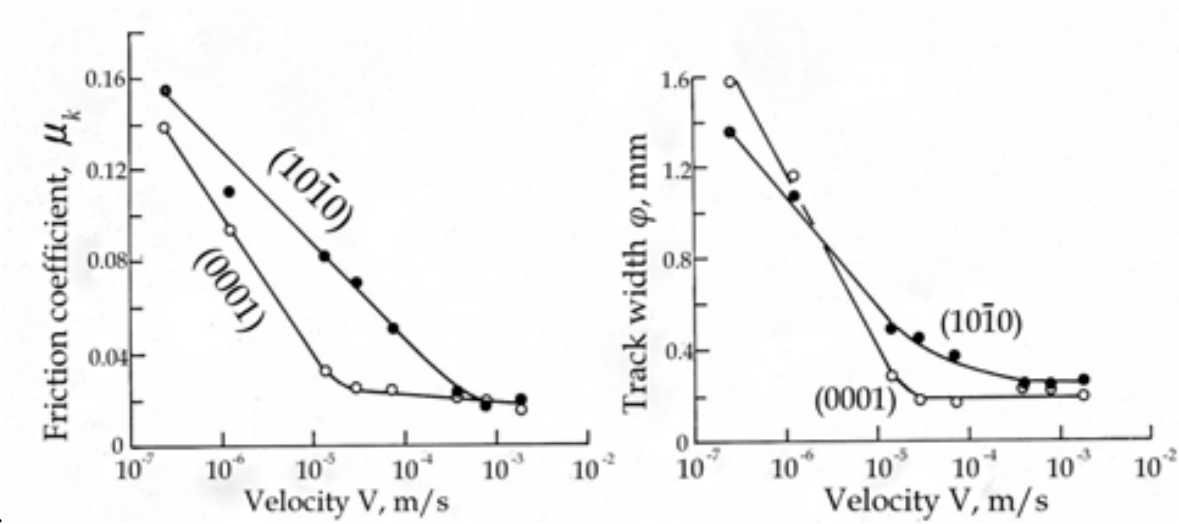
Fig. 7. (a) Dependence of friction an velocity, and (b) width of a sliding track against load. Temperature -10°C, Load 14N, Diameter of slider 6.4mm (after Tusima,1977)

temperature approaches its melting point. This increase may be closely to the increase in the width of the sliding track as shown in Fig. 8(b). We may conclude that the increase in the friction is caused by the ploughing of ice at the contact area. It should be noted that the minimum friction shifted to a higher temperature as the friction velocity was reduced. For example, it was at -4°C and -2°C when the velocity was 1.5×10^{-5} and 1.2×10^{-6} m/s, respectively.
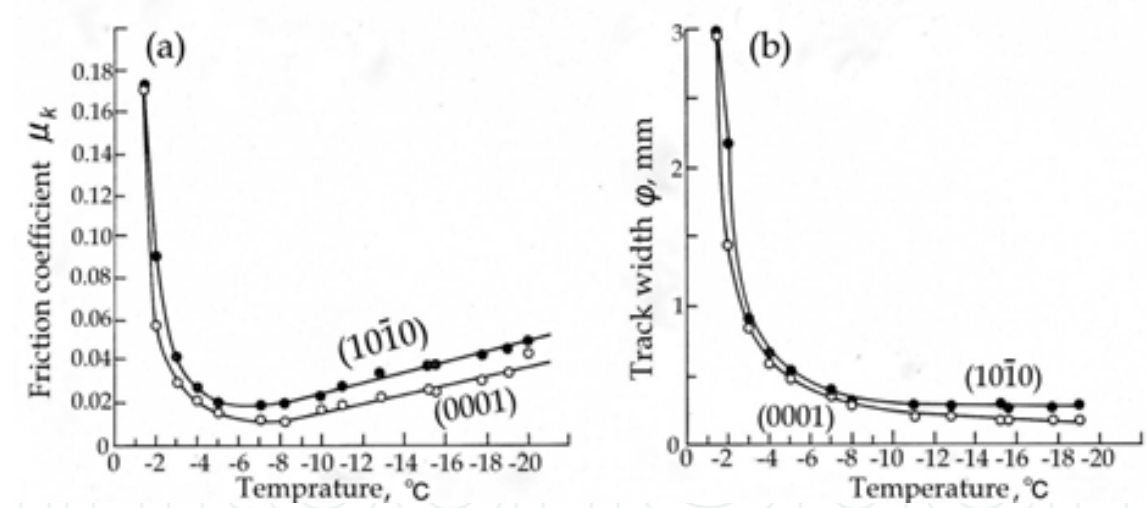
Fig. 8. (a) Dependence of friction on temperature, and (b) dependence of the width of the sliding track on temperature (after Tusima, 1977).

4.1.5 μ_k -V-W diagram

Dependence of the friction coefficient on the sliding velocity and load for a prismatic and a basal plane of ice are respectively summarized in Fig. 9(a) and (b). The coefficient μ_k ranged from 0.005 to 0.16. Though the friction varies with velocity, load and temperature, it is much smaller than those observed for metals. The coefficient μ_k is much smaller for the basal plane than for the prismatic plane for any experimental conditions. This may be due to the fact that the ice is very strong when it is compressed perpendicular to the basal plane, while it is very weak against a shearing force, which will be discussed later again.
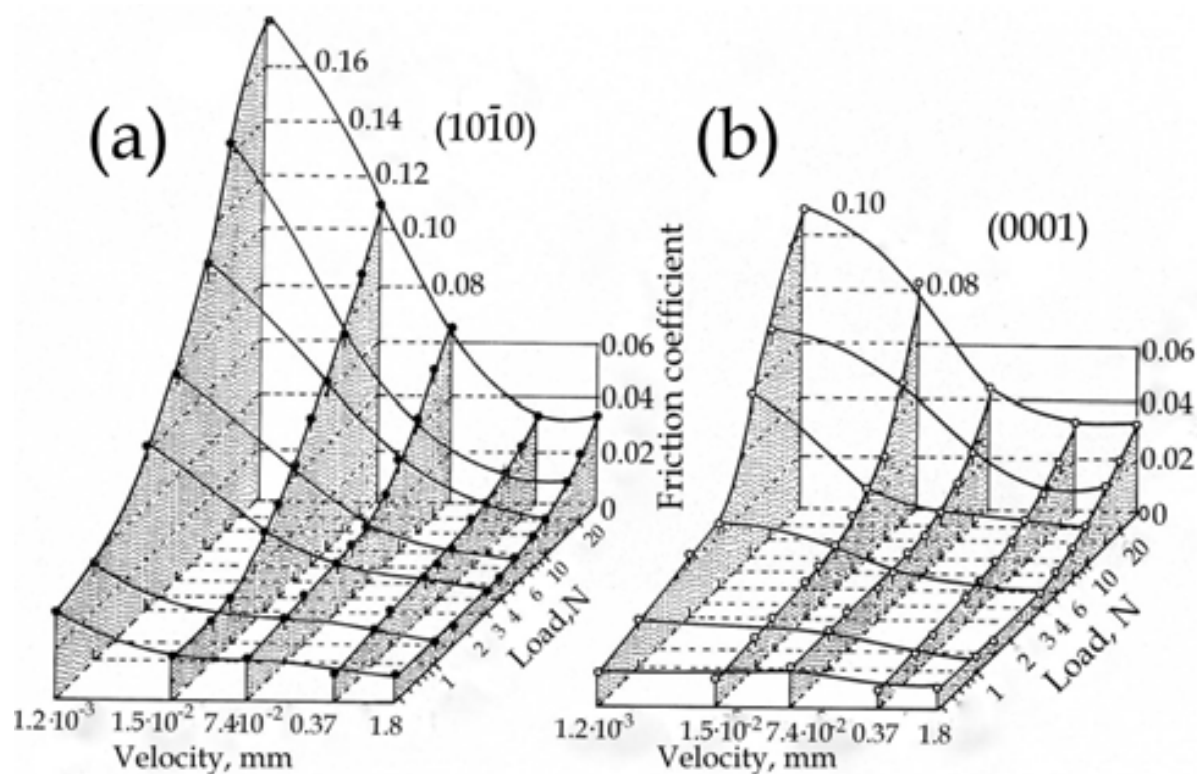
Fig. 9. μ_k-V-W diagram, (a) for a prismatic plane, and (b) for a basal plane.
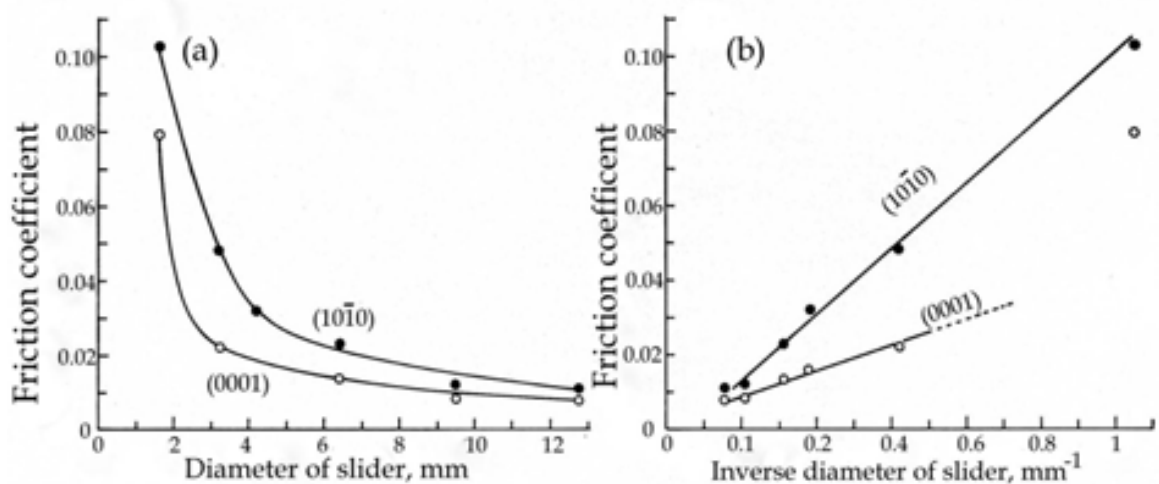Temperature -10°C, Slider diameter 6.4mm(after Tusima, 1977).

Fig. 10. Size effect of a steel ball on the friction of ice against diameter (a) and inverse
diameter (b). Solid circle on the prism plane ($10\bar{1}0$); open circle on the basal plane (0001).
Temperature -10°C, velocity 7.4x10⁻⁵ m/s, load 4.8N. (after Tusima,1977)

4.1.6 Effect of the size of ball

The degree of ploughing of ice by a steel ball may become larger as the ball becomes smaller
in size. In order to examine the size effect of ball on friction of ice, steel balls of different
diameters ranging from 1.6 to 12.7 mm were used as a slider. The results obtained are
shown in Fig. 10. As was expected, μ_k increased with the decrease in size of the ball for a
smaller range of diameters than 9.5 mm when the load, the sliding velocity, and the

temperature were 4.8 N, 7.4×10^{-5} m/s and -10°C, respectively. However, μ_k remained unchanged when a steel ball larger than 9.5 mm in diameter were used and this will give pure shear friction.

μ_k-V-1/R diagram is shown in Fig. 11. R is diameter of slider. Fig. 11 shows the same relation to Fig. 10.
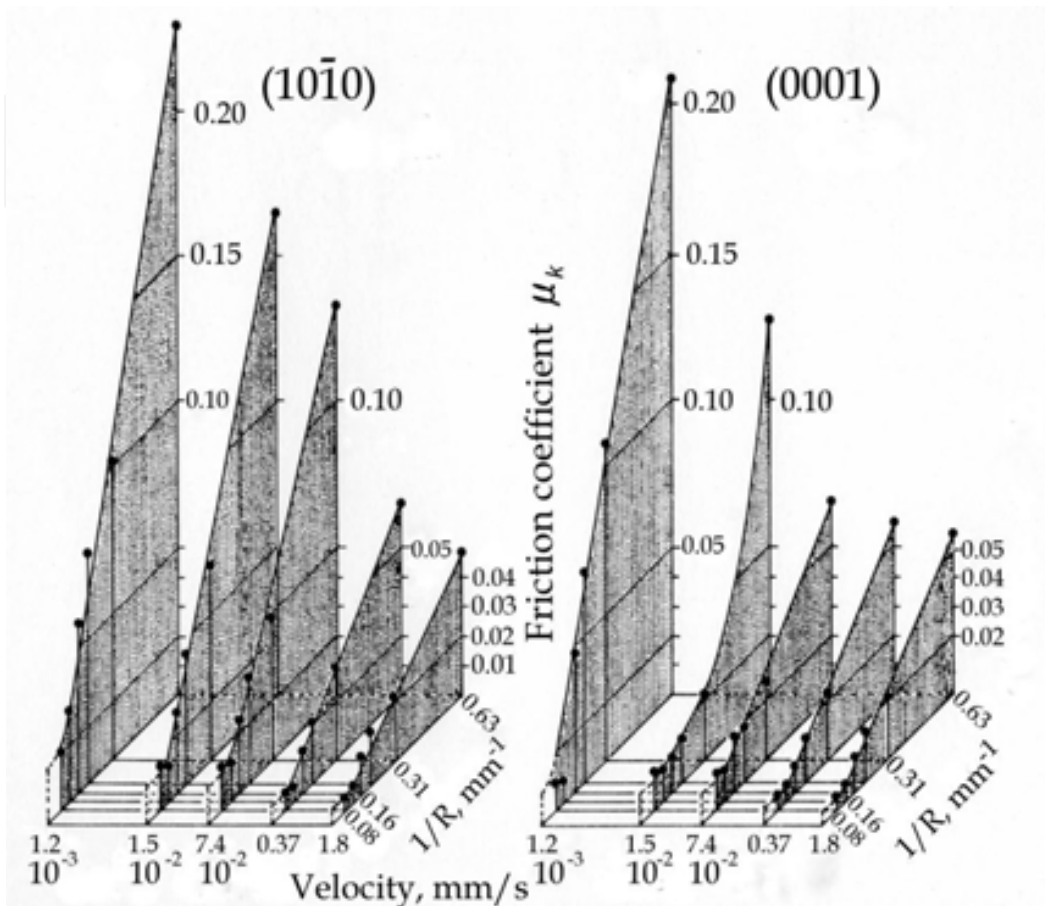

Fig. 11. μ_k-V-1/D diagrams, on prism plane (10$\bar{1}$0) at left; on basal plane (0001) at right. Temperature : -10°C; load: 4.75 N.

1/R→0 correspond to pure shear friction and gives possibility the determination of shear strength s.

4.1.7 Effect of other crystallographic plane of ice on friction

Fig. 12 shows μ_k against inclined basal plane. The μ_k were roughly constant between 0 to 60°, but μ_k increased to high value in between 70 and 90°. Of course, μ_k changes by sliding orientation even on same plane.

4.1.8 Feature of frictional track of ice

Observation of frictional track of ice as shown Fig. 13 may give information as the solid friction mechanism. Ice has high vapor pressure and the disturbed region was changeable by sublimation, annealing and recrystallization etc. Therefore, the track must be observed quickly after sliding. Fig. 13 shows the groove, recrystallizaion, microcrack, plastic deformation etc.
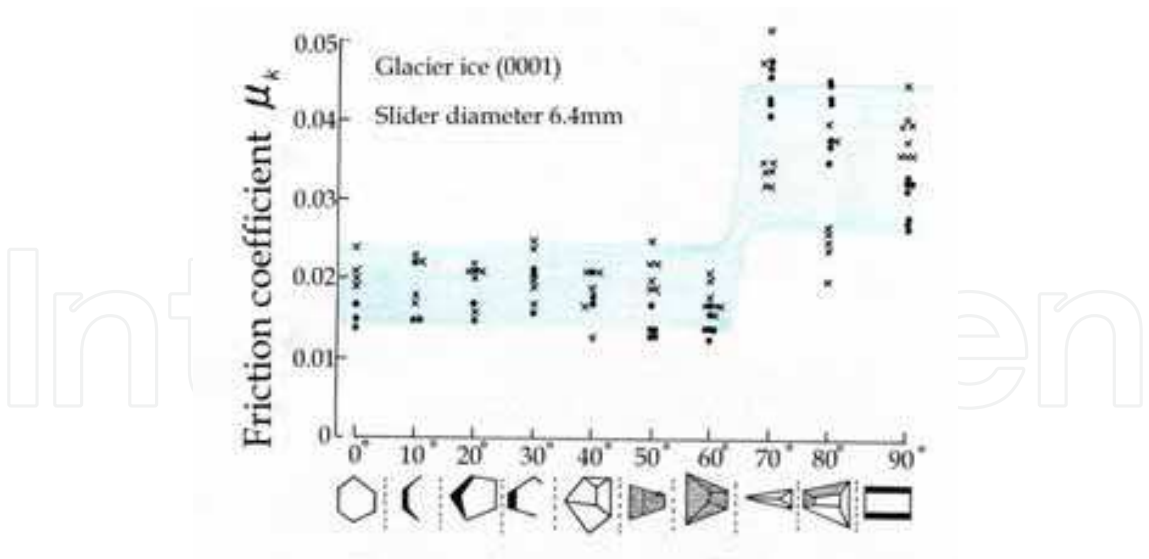
Fig. 12. Coefficient of kinetic friction μ$_k$ against angle of basal plane for ice surface.
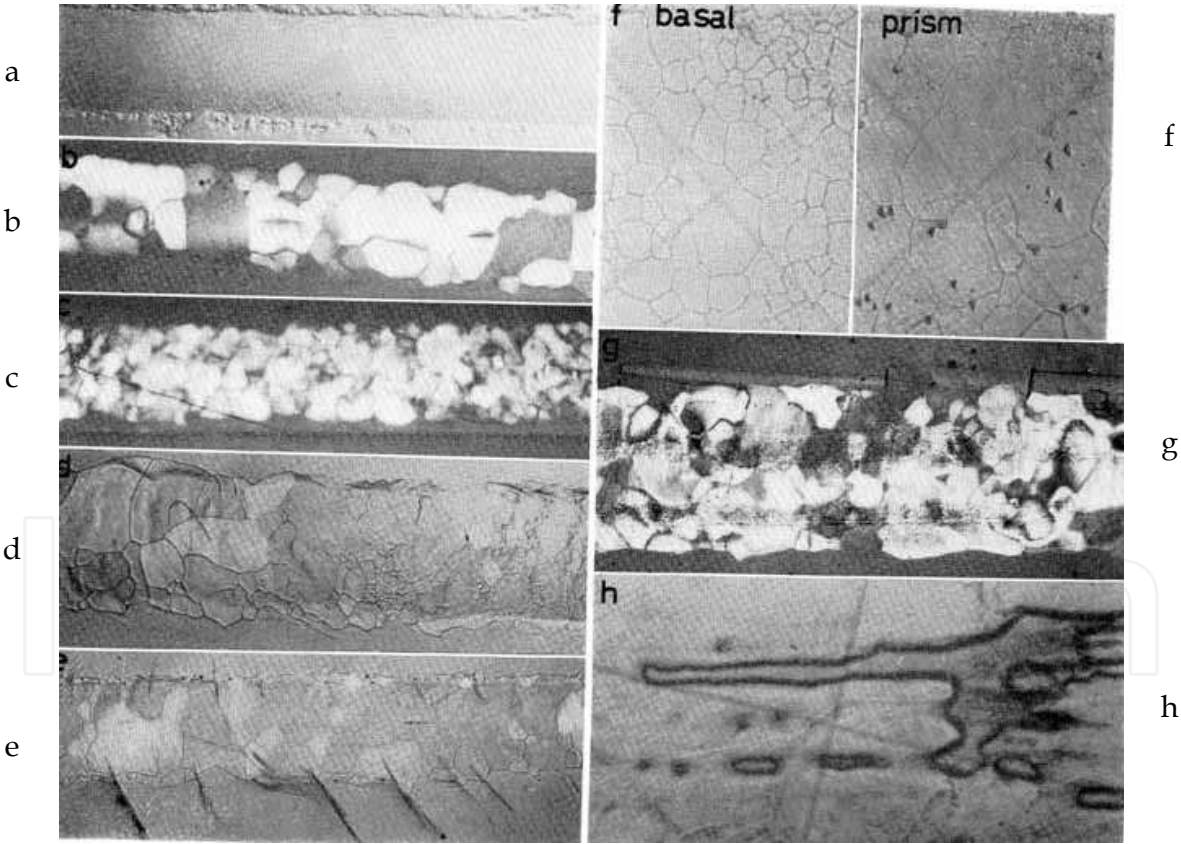Temperature -10°C, velocity 7.4x10^{-5}m/s, load 4.7N.

Fig. 13. Frictional track of ice a : low load, b : recrystallization on prism plane of ice,
medium load, c : recrystallization and crack, heavy load, d : recrystallization of basal plane
of ice, medium load, e : recrystallization and crack of basal plane of ice, heavy load, f :(left)
recrystallization of basal plane, (right) recrystallization of prism plane, g : small angle grain
boundary, crack and recrystallization of prism plane, a~g at the temperature of -10°C, h :
rarely pattern like melting at -30°C

It was found that friction on ice is very low even at a very small velocity; namely the μ_k varied from 0.005 to 0.16 for velocities ranging from 1.8×10^{-3} to 1×10^{-7} m/s. Such low friction on ice at extremely small velocities cannot be explained by frictional heating.

The temperature rise of ice, ΔT, due to friction can be expressed as follows (Bowden & Tabor, 1950):

$$\Delta T = \mu_k WV/[4a(k_1+k_2)], \tag{3}$$

Where μ_k is the coefficient of friction, W the load applied, V the friction velocity, a the radius of the contact area and k_1 and k_2 the thermal conductivities of slider and ice. The maximum temperature rise ΔT predicted from this formula is only 0.3 deg even when the maximum values of load W and friction velocity V used in the present experiment and the maximum value of friction coefficient 0.2 were substituted into the formula. It is obvious that the temperature rise due to frictional heating cannot cause melting of the ice.

It was also confirmed that melt water cannot be produced at the contact surface by pressure except at high temperatures.

According to adhesion theory, the frictional force F on ice can be divided into the shear resistance F_s and the ploughing resistance F_p: $F=F_s+F_p$. The coefficient of friction $\mu_k(=F/W)$ can, therefore, be written as the sum of the shear term μ_S and ploughing term μ_p: $\mu_k=\mu_s+\mu_p$. According to Bowden & Tabor (1950), F_s and F_p were respectively given by:

$$F_s=k\pi\varphi^2 s/4, \quad F_p=\varphi^3 p/6R^2 \tag{4}$$

where s and p are respectively the shear and the ploughing strength of ice, R is the diameter of slider, φ is the width of the sliding track and k is a constant. The coefficient of friction μ_k can, therefore, be expressed as

$$\mu_k = k\pi\varphi^2 s/4W + \varphi^3 p/6WR \tag{5}$$

As the first term, $k\pi\varphi^2/4W$, and a part of the second term, $\varphi^3/6WR$, are constant for given load and a temperature, this formula can be simply expressed as

$$\mu_k =A+a/R \tag{6}$$

where A and a are constant.

A linear relation was actually obtained between μ_k and $1/R$ be in the experiment on the effect of slider size (Fig.10(b)). This is evidence that the adhesion theory can be adopted for the friction of ice.

The values of s and p were estimated as follows: As described when considering the size effect, only a shear deformation took place in the contact area when a slider of diameter $R \geqq 9.5$mm was used.

The shear strength s is, therefore, given by $s = 4F/k\pi\varphi^2$, where the value of k is 0.8 as mentioned before. The value of the ploughing strength p was estimated from Equation (5).

Since $\mu_p=\varphi^3 p/6WR$, the values of p can be obtained by substituting values of φ, W and R used in the experiment. The values thus obtained for s and p are 0.7 MPa and 75 MPa, respectively. By substituting into the Equation (3) these values of s and p, together with the experimental data obtained. These values are summarized in Table 4, together with some experimental data obtained for various load. As seen in this table, the coefficient of shear friction μ_s does not vary with load, while that of ploughing friction μ_P increases markedly

with the increase in the load. The predicted values of $\mu_k(=\mu_s+\mu_p)$ agreed fairly well with those obtained by experiment for any load that ranged from 1.4 to 41 N as seen from the last column of Table 4 in which the ratio of $(\mu_s+\mu_p)$ to μ_k observed in the experiment was given. The fact that the predicted value based on the adhesion theory agreed well with those observed in the experiment. It should be emphasized that ice still exhibits a very low friction even though the ploughing effect is fairly large at very small sliding velocities.

4.2 Anisotropy of friction to sliding direction on same crystallographic plane of ice

4.2.1 Anisotropy in friction and track width on prism planes (10$\bar{1}$0)

Friction was measured every 10° on a prism plane (10$\bar{1}$0). No abrasive fragmentation occurred along the track, thus, friction tracks formed only by plastic deformation of ice.
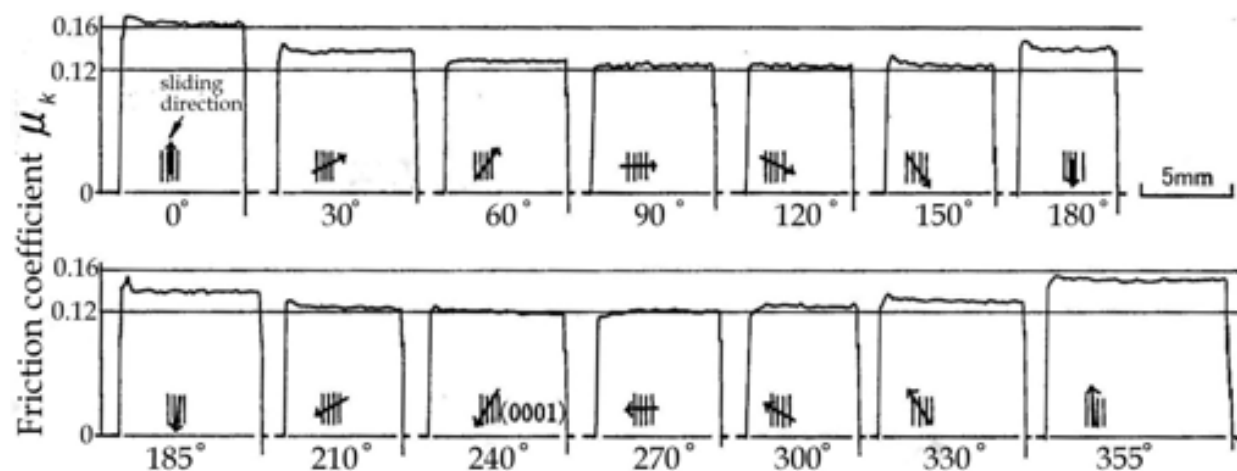

Fig. 14. Friction curve on prism plane (10$\bar{1}$0). Load : 6.9N, velocity : 7.4×10^{-5}m/s, temperature : -25°C, slider diameter 2.34 mm, allow shows direction of sliding.

Fig. 14 shows the record of friction as a function of the angle θ from the [10$\bar{1}$0] direction. Other parameters of the test were: temperature, -25°C; velocity, 7.4×10^{-5} m/s; applied load, 6.9 N; diameter of the slider, 2.34 mm. The coefficient μ_k reached its maximum in the [10$\bar{1}$0] direction and a minimum along [0001]. The value of μ_k ranged from 0.12 to 0.16, the ratio maximum/minimum being 1.3.

Fig. 15 shows photographs of the terminal areas of friction tracks produced by a slider on the prismatic surface at -21°C. The deformed regions are extended beyond the sides of the track revealing mainly horizontal slip lines and microscopic crack produced by the slider (2.34 mm in diameter). Fig. 15(b) shows a deformed bulge that moved in front of the slider parallel to the basal plane. Note that many cracks which are oriented normal to the basal planes propagate ahead of the slider, but that no significant deformation areas were found at the sides of track. The deformed area which formed near the terminus when the slider was moved diagonally to the basal plane (Fig. 15(c)) showed an intermediate pattern between those of Fig. 15(a)and (b). Note that many cracks were created normal to slip lines oriented in the [10$\bar{1}$0] direction.

From inspection of these photographs, we may conclude that when slider is moved parallel to the basal plane (Fig. 15(b)), comparatively higher values of μ_k may be obtained because of bulge formation in front of the slider.
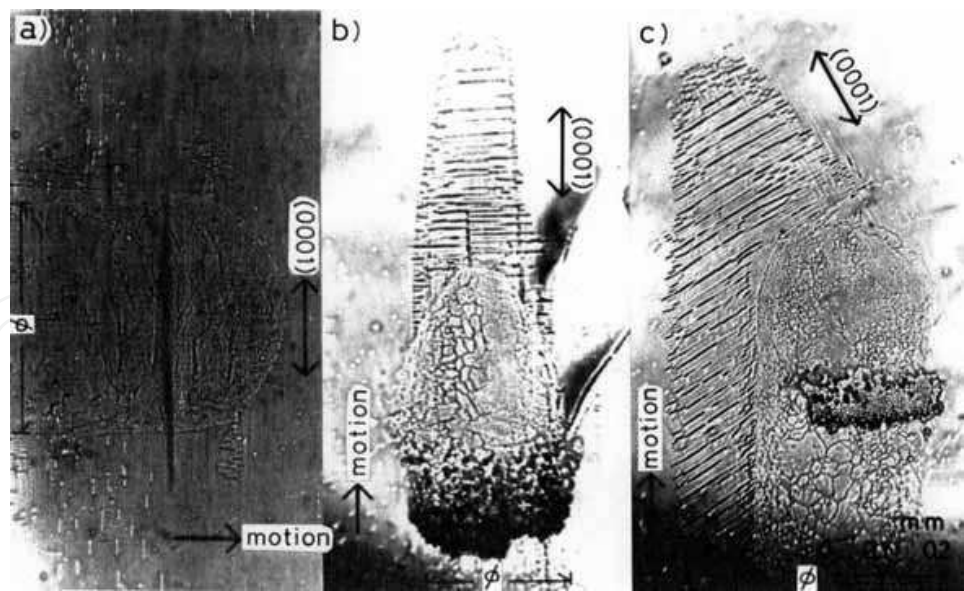
Fig. 15. Traces in track ends of friction on (10$\bar{1}$0). Sliding directions: (a) [0001]; (b) [10$\bar{1}$0]; (c) 30°from [0001]. Note that the basal slip lines extend parallel to [10$\bar{1}$0] and there is a dark line normal to the slip lines. Load 6.7N, velocity 7.4x10^{-5} m/s, Temperature -21°C, →sliding direction. (after Tusima, 1978)
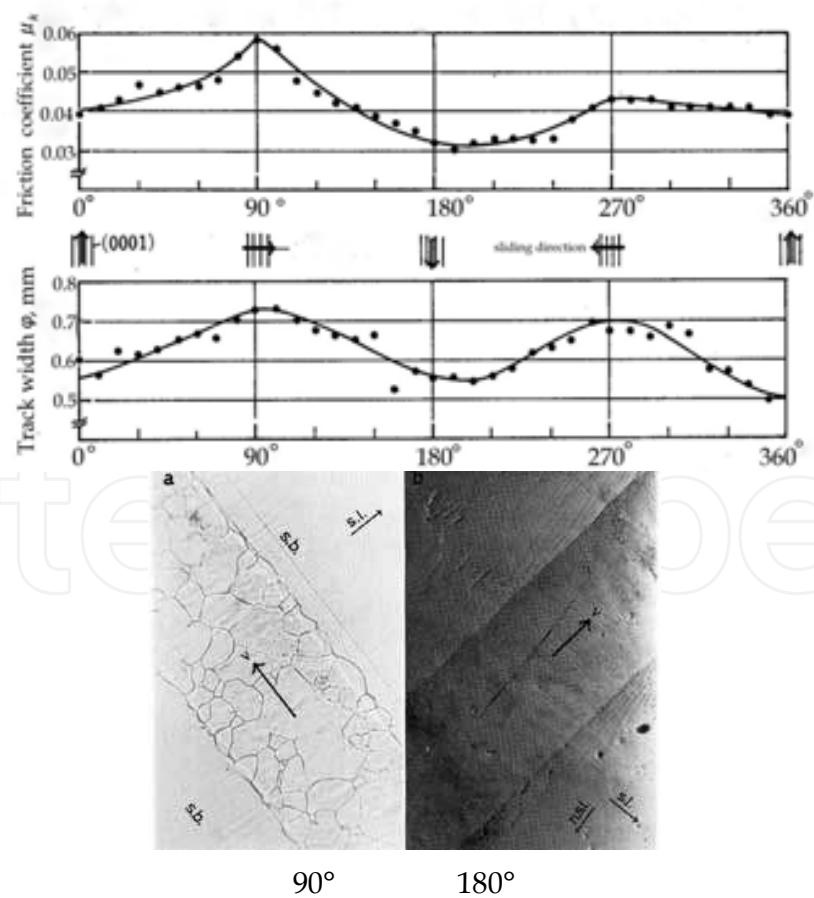

90°   180°

Fig. 16. Anisotropies in friction μ_k and track width f on (10$\bar{1}$0). Temperature: -10°C; load: 14.4N; velocity :6×10^{-5} m/s; slider: 6.4 mm in diameter. (after Tusima, 1978)

The friction coefficient reversed at temperatures of -10°C and above shown in Fig. 16. For this experiment, the temperature was -10°C, the velocity was 6.0×10^{-5} m/s, the load was 14.4 N, and the slider diameter was 6.4 mm. The maxima of the friction coefficient and the track width were observed to be in the same direction, which contrasts with the results obtained at temperatures of -21°C and below.

4.2.2 Anisotropy in friction on inclined surfaces to (0001)

As shown in Figs. 14 and 16, a significant amount of anisotropy in the μ_k value was found on the prismatic surface where the orientation of the basal planes in ice are normal to the test surface, but on the basal surface itself no such anisotropy was observed. This may suggest that the μ_k value measured on a given surface of ice depends on the relationship between the sliding direction and the orientation of the basal planes in ice. Fig. 17 shows anisotropies in the μ_k value and the track width measured on a surface of ice cut diagonally against the basal plane. In this sample the (0001) plane was inclined at approximately 30° to surface. The abscissa is the angle of revolution of the test surface against the slider. When the angle of the test surface was fixed at 0°, the slider moved parallel to the basal plane on the surface.
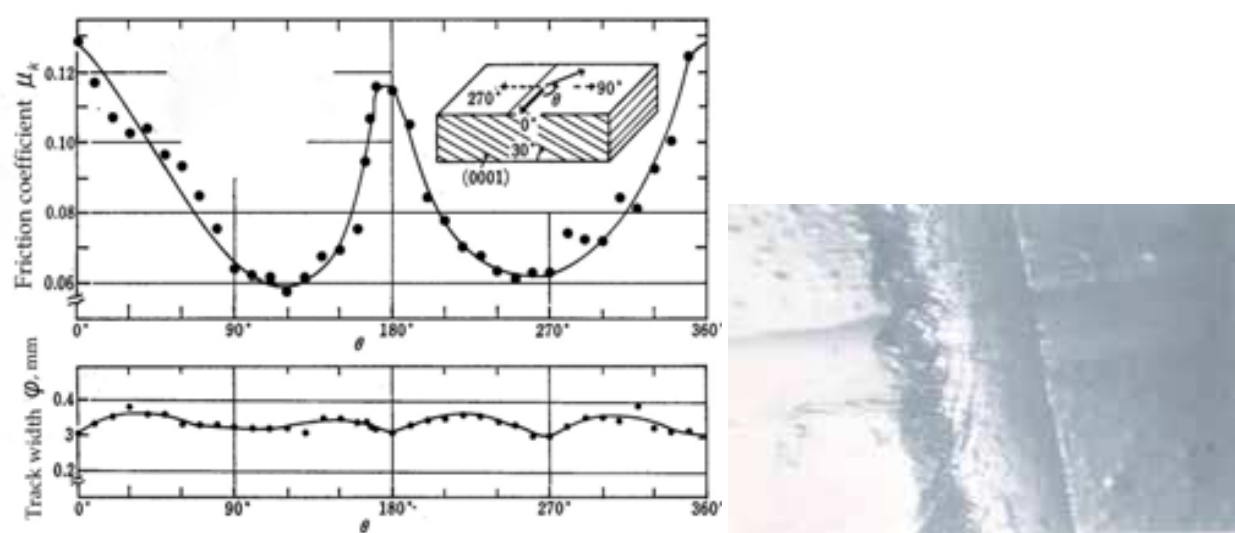

Fig. 17. Anisotropies in friction μ_k and track width φ on (0001) declined at 30°. Temperature: -20°C; load: 6.9N; velocity : 7.4×10^{-5} m/s; slider: 2.34 mm in diameter (right) frictional track (after Tusima,1978)

As shown in Fig. 17, two maxima in μ_k appeared at 0° and 180° (where the slider moved in parallel with the basal plane), but two minima appeared at about 120° and 260° (where the slider moved nearly perpendicular to the basal plane). Although values of μ_k changed significantly with sliding direction, a slight variation in track width was observed.

As seen above, μ_k values on the prismatic plane in diagonally cut surfaces depended on sliding direction. In order to interpret the observed anisotropy, the friction track produced on the specimen surfaces was observed using optical microscopy. According to our observation, recrystallization, cleavage fissures, microcracks, slip lines, and small-angle boundaries were found to have formed along a friction track.

The coefficient of kinetic friction μ_k may be explained solely in terms of prismatic deformation of ice. According to the adhesion theory, μ_k is given by

$$\mu_k = (k\varphi^2 s/4 + k'\varphi^3 p/6R)/W \qquad (7)$$

where s is the interfacial shear strength between ice and slider, p the ploughing strength of ice, R the diameter of slider, W the applied load on the slider, φ the width of track produced by friction, k and k' the shape factors (for the sake of convenience, we shall assume that k = 0.8 and that k' =1 (Tusima ,1977).

As seen in Equation (1), μ_k is composed of two terms, the first terms, interfacial shear and the ploughing effect of the slider.

Fig. 10 shows μ_k, measured on the prism surface, as a function of temperature and reciprocal slider diameter. The velocity of the slider and value of applied load are indicated on the figure. μ_k is inversely proportional to the diameter of the slider, suggesting that Equation (1) can be used in the interpretation of our results. According to Equation (5), the effect of slider ploughing disappears if the slider can be considered to have an infinite diameter. The largest slider diameter used in our experiments was 12.5 mm. If we assume that the ploughing term is negligible in value of μ_k measured with this slider, then we can plot the shear strength of ice calculated by the shear term in Equation (4) as a function of temperature (Fig.18).

From Equation (5), the ploughing strength p of ice is expressed as

$$p = 6R(\mu_k W - k\varphi^2 s/4)k'\varphi^3 \qquad (8)$$

Since the s is known from Fig. 18, if we substitute numerical values for μ_k and φ measured in the various sliding directions into Equation (8), we can estimate p as a function of direction. Fig. 19 shows the p anisotropy measured on the prism surface ($10\bar{1}0$), p is one of the indices used to express ice surface hardness.
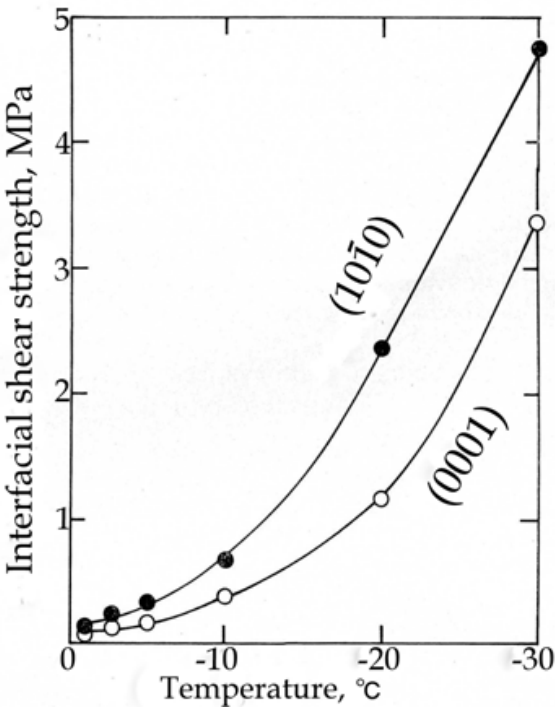

Fig. 18. Interfacial shear strength between ice and steel, plotted against temperatures, for planes ($10\bar{1}0$) and (0001). (after Tusima, 1978)
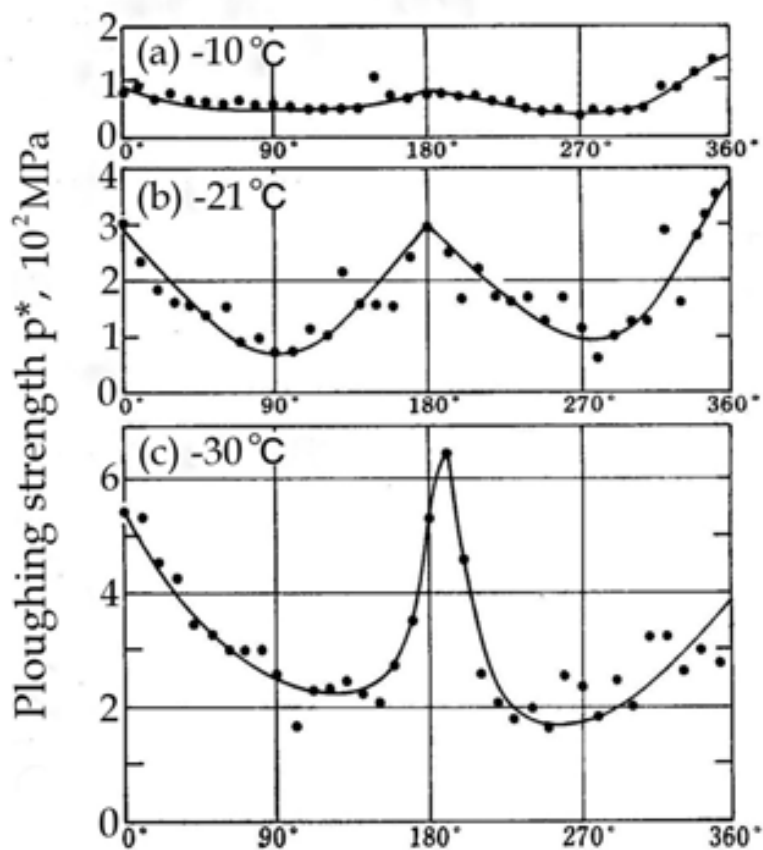
Fig. 19. Ploughing strength on (10$\bar{1}$0) calculated from friction coefficients and track width.
(a) Temperature: -10°C; load: 14.4N; velocity: 6.0×10^{-5} m/s; slider: 6.4 mm in diameter. (b) Temperature: -21°C. (after Tusima, 1978)

Butkovich (1954) and Offenbacher & Roselman (1971) measured the hardness anisotropy of ice single crystals. Offenbacher & Roselman found that, on the prism plane, Knoop hardness measured in the direction normal to the basal plane was smaller than the value obtained parallel to the basal plane. The p anisotropy obtained by the present author seems to agree roughly with the Knoop-hardness values obtained by Offenbacher & Roselman (1971).

The appearance of a maximum in the value of p along [10$\bar{1}$0] may be understood by the bulge formed ahead of slider (Fig.15(b)). The anisotropy in the coefficient of kinetic friction on the prism surface of ice can be explained in terms of the anisotropy in p and φ. Therefore, the anisotropy in μ_k depends on $p\varphi^3$. The value of p and φ showed maxima or minima in the sliding direction [10$\bar{1}$0] and [0001]. Thus, the frictional anisotropy μ_k[10$\bar{1}$0]/μ_k[0001] may be proportional to

$$(p[10\bar{1}0]/p[0001]) \times (\varphi\,[10\bar{1}0]/\varphi\,[0001])^3.$$

These values are summarized for various temperatures in Table 5. When the ratio of $p\varphi^3$[1120]/$p\varphi^3$[0001] becomes smaller than 1, frictional anisotropy is dominated by the track-width anisotropy. When the ratio is larger than 1, frictional anisotropy is dominated by ploughing-strength anisotropy. Both results agree with the experimental observations. The anisotropy in friction can be well explained by the anisotropies in ploughing strength and track width.

Temperature °C	$(\varphi\,[10\bar{1}0]/\varphi\,[0001])^3$	$p[10\bar{1}0]/\,p[0001]$	$\mu[10\bar{1}0]/\mu[0001]$	
			calculated	observed
-10	0.40	1.8	0.72	0.67
-21	0.39	3.4	1.3	1.3
-30	0.51	2.8	1.4	1.2

Table 5. The ratio of track width, ploughing strength, and friction coefficient between directions of $[10\bar{1}0]$ and $[0001]$ for different temperatures on prism plane $(10\bar{1}0)$. (after Tusima, 1978)

Friction anisotropy on the basal (0001)and prism $(10\bar{1}0)$ planes of ice was measured as a function of track width, the amount of plastic deformation caused by frictional sliding, as so on. It was found that, for the prism planes, friction reaches a maximum in the $[10\bar{1}0]$ sliding direction on the $(10\bar{1}0)$ planes and in the $[10\bar{1}0]$ direction on the $(10\bar{1}0)$ planes. Friction is at a minimum in the $[0001]$ direction for both planes at temperatures below -19°C. At temperatures of -10°C and above, the maximum friction was observed in the $[0001]$ direction and the minimum in the $[10\bar{1}0]$ direction for $(10\bar{1}0)$ planes, and in the $[10\bar{1}0]$ direction for $(10\bar{1}0)$. A remarkable friction anisotropy was $(10\bar{1}0)$ planes, and in the $[10\bar{1}0]$ direction for $(10\bar{1}0)$. A remarkable friction was observed on pyramidal planes, although track-width anisotropy was very small. No marked anisotropy in friction was observed on the basal plane.

The width of the frictional track also varied with the sliding direction on the prism plane; that is, it was at a maximum along $[0001]$ and reached minima along $[10\bar{1}0]$ for the $(10\bar{1}0)$ plane and along $[10\bar{1}0]$ for the $(10\bar{1}0)$ plane, independent of temperature.

4.3 Friction of plastic balls on ice
### 4.3.1 Experimental method and samples
The apparatus shown in Fig. 2 was used measurements μ_k of polymer balls on a flat plate with crystal orientation (0001) of single-crystal ice.

Polymer balls obtained from Urtraspherics Co.Ltd., USA, were: polymethylmethacrylate (PMMA), polytetrafluoroethylene (PTFE, Teflon), polypropylene (PP), polyethylene (PE), polyamide (PA, Nylon), polyacetal (POM), polycarbonate (PC) and polystyrene (PS). They were also cleaned in the same manner as a steel and tungsten-carbide ball (TC) without acetone.

4.3.2 Friction and frictional track of plastic balls on ice
The relations of μ_k to the load applied are shown in Fig. 20. The values of μ_k which were roughly constant for loads except for PMMA, were high, from 0.04 to 0.15. Constancy in μ_k follows from softness of plastics, compared with ice.

Plastic ball except PMMA showed frictional track wider than steel ball and its μ_k were greater than steel ball. Ice surfaces were disturbed markedly as shown in Fig. 21. Fig. 21 shows many streak, abraded particle, recrystallization, crack. The value of μ_k was the greater, surface damage of ice the heavier.
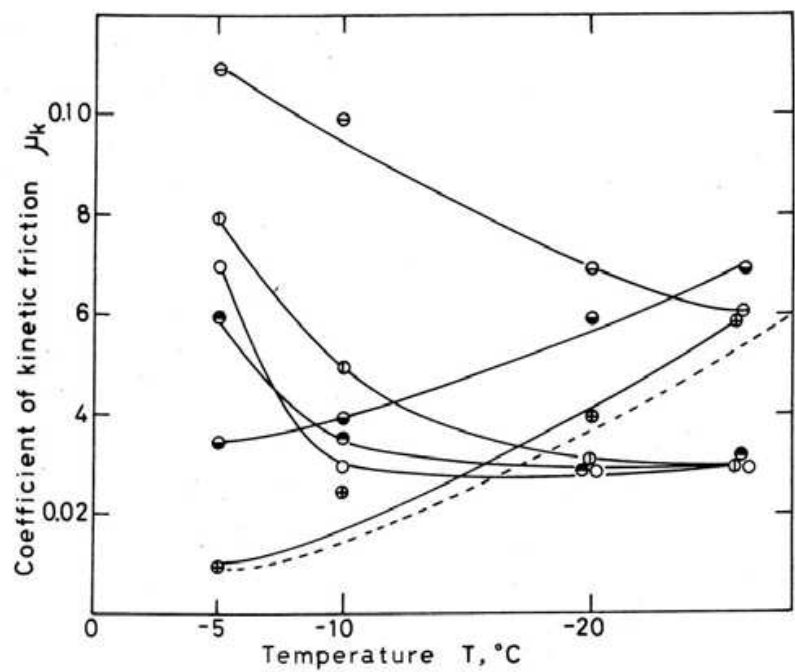
⊖:PA; ⌀:PE; ○:PTFE; ◐:POM; ◑:PP; ⊕:PMMA;

Fig. 20. Dependence of friction on temperature on basal plane (0001) of ice. Load: 4.75 N; velocity: 7.4x10⁻² mm/s; diameter of slider: 6.4 mm. broken line: steel ball. (after Tusima, 1980)
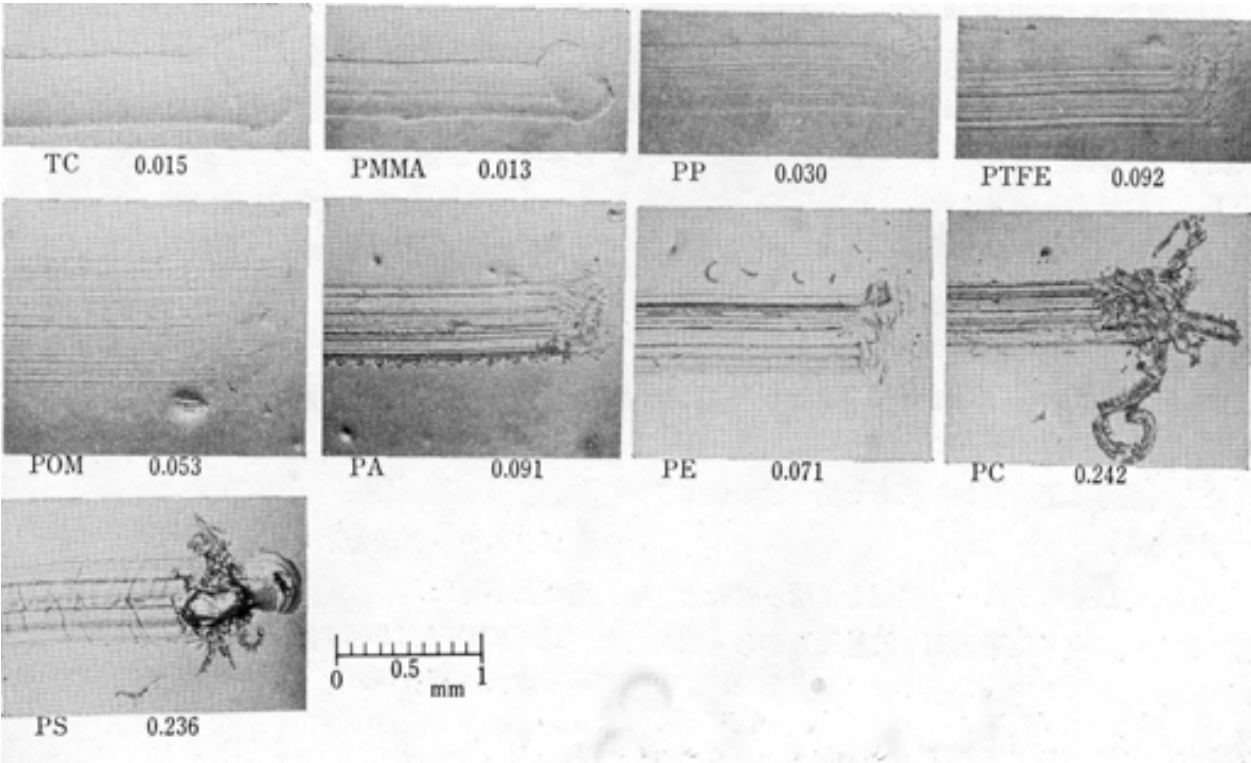

Fig. 21. Trace of a track marked by a slider ball on basal plane (0001) of ice. Figure under each picture shows coefficient of kinetic friction. Temperature:-5ºC, load: 47.5N, velocity: 7.4x10⁻²mm/s, diameter of a slider: 6.4mm (after Tusima,1980)

5. Other frictional properties of ice and snow

5.1 Sliding of speed-skate on speed-skate ice-rink

We knew that friction of ice had a minimum value in (0001) plane of ice at sliding of tungsten carbide ball on single crystal of ice. This relation was confirmed with sliding of speed skate as shown in Fig. 22 and Table 6. At first, ice plates with (0001) was connected in linearly, and test course gained of 1 m long.
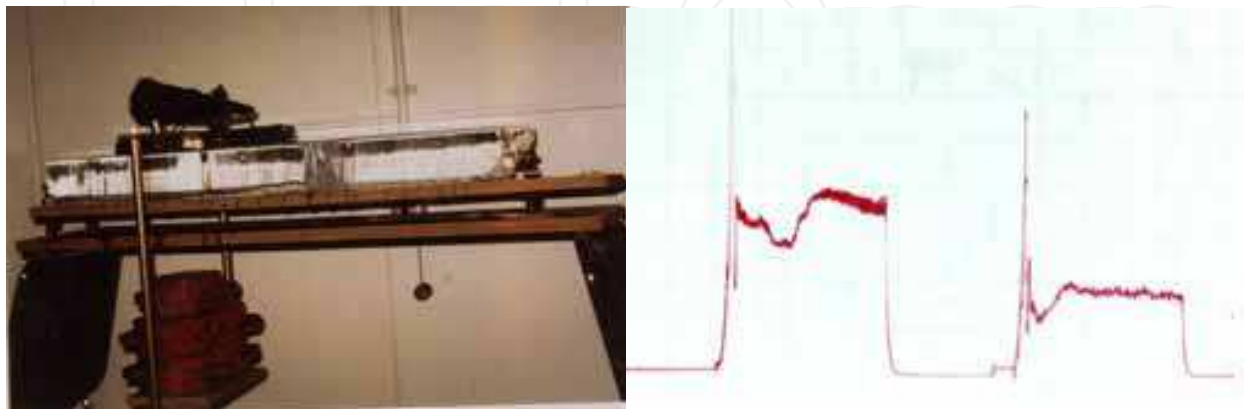
Fig. 22. Sliding test by real skate left: μ0.031 on polycrystalline ice, right: μ 0.021 on (0001) of ice. Temperature: -10ºC, velocity :0.05m/s, load: 550N

Ice surface cut carefully by microtome and one blade of speed-skate was slid by pulling constant speed. Friction force detected electrically by load cell and recorded on paper as shown in Fig. 22. Friction coefficient was 30% smaller on (0001) plane of ice than poly-crystalline commercial ice.

Next, rink test is planned to control (0001) ice surface for skating rink because low friction of (0001) is confirmed on ice sample. Numerous large single-crystal of ice (diameter 0.1~0.15m, long 0.3~0.4m) was grown in direction parallel to c-axis in temporary prepared cold room of length 190m (Fig. 23). Thin plate of single-crystal (thickness 7mm) was cut by band-saw and the plate was pasted on ice-rink and grown by repeatedly supply a small amount of tepid water (40ºC). Vertical thin section of obtained ice was shown in Fig. 25, left figure was view transparent light and right figure the view of cross polaroid. The crystallographic orientation was maintained constant in growing process of oriented over growth. Normal rink is polycrystalline as shown in Fig. 24.

Preliminary test was made in short track of skating rink. Test skate with speed-skating brades was started at the initial speed, v_0, of 1m/s. The distance, ℓ, until stop was measured. Average friction coefficient, μ, was determined as $\mu = v_0^2/2g\ell$.

Obtained results is shown in Table 6 at initial velocity about 1 m/s and ice temperature -3ºC, load of 392N. Friction coefficient 0.0064 on (0001) is compared 0.0081 on normal ice rink, the coefficient decreased 21% in (0001) than one of polycrystalline ice rink (normal rink).

Next, main test repeated in full scale speed-skating rink at Olympic Memorial Arena "M-Wave" Nagano, Japan. In this case, all surface round, 400m, changed to (0001) of ice. Therefore, comparison of μ was tried between (0001) ice of speed- skate rink and poly-crystalline ice of virgin ice-hockey rink on same floor. Table 6 shows comparison (0001) rink to normal rink at initial starting velocity 1m/s. Friction coefficient 0.0038 on (0001) was 16% smaller than 0.0045 on normal rink. Measured coefficient of friction when initial velocity

changed in the range 0.2~3.5m/s was low as 0.003~0.008. At lower than 1m/s, the coefficient increased with decreasing velocity though the value was 0.004~0.006 in higher initial velocity range than 1 m/s.

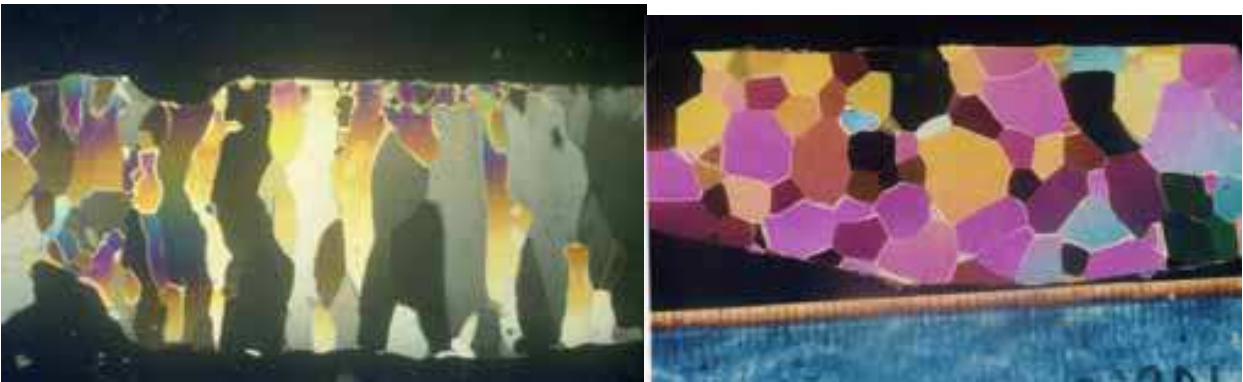Fig. 23. Ice making on ice-stalagmite Right: Horizontal section of ice-stalagmite

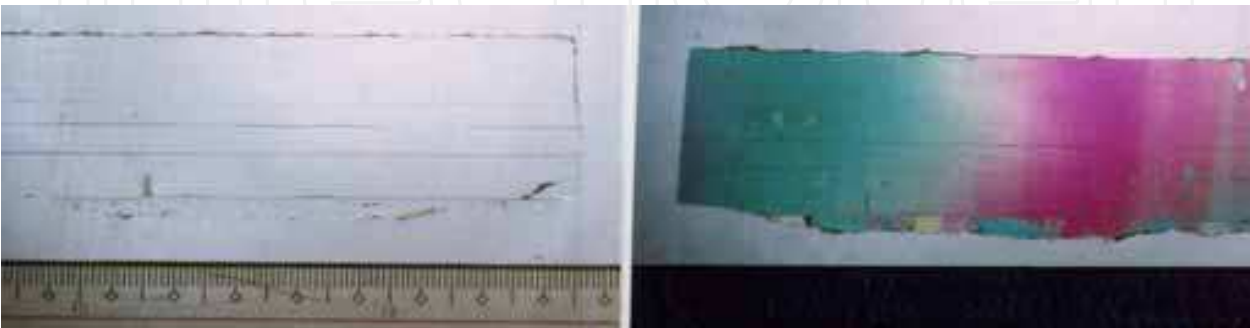Fig. 24. Normal rink ice left: vertical section, right: horizontal section (scale: minimum division 1mm)

Fig. 25. Ice-stalagmite rink controlled to (0001) surface, Vertical section. Scale: minimum division 1mm

Fig. 26. Test skate by catapult

Frictional melting does not occur in these conditions, any water did not exist. Pure solid friction will attain in these test, therefore it is considered to be reflected in sliding the properties of crystallographic plane of ice. If water concern sliding on ice, the water should be prepared by the frictional melting. The decrease of friction means the decrease of heat, therefore it is impossible to melt in extremely small friction as sliding of speed-skate shown in Fig. 27. It is concluded that anisotropy of friction by crystallographic plane of ice caused in pure solid friction without liquid.
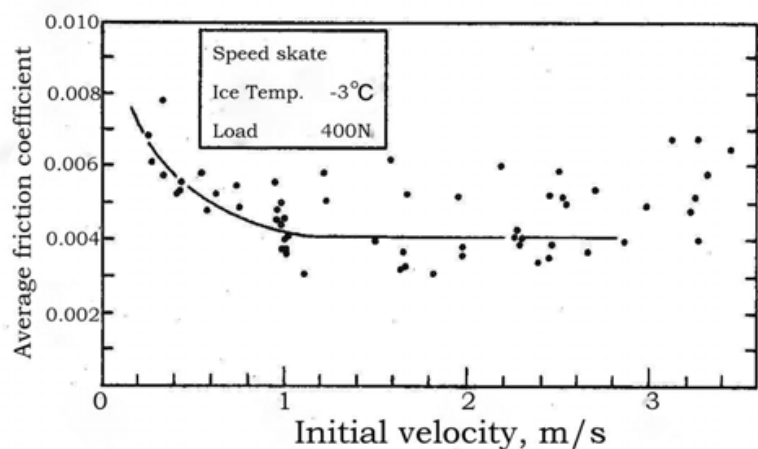
Fig. 27. Relation between initial velocity and average friction coefficient (M-wave, Speed-skating rink, Nagano, Japan) (after Tusima,2009)

Temperature	-3.1°C	-4.1°C
	Speed skate rink (0001)	Ice hockey rink polycrystalline
	0.0040	0.0046
	0.0037	0.0044
	0.0036	0.0046
	0.0037	0.0042
	0.0040	0.0045
mean	0.0038	0.0045

Table 6. Comparison of friction coefficient between test ice (0001) and normal one (M-wave, Nagano) Load: 294N, Initial velocity: 0.9~1.1m/s. (after Tusima et.al.,2000)

It is noticed the increase of μ the decreasing initial velocity. This μ - v relation will give the explanation of curl of curling rock.

5.2 Tribology of curling stone on pebbled ice sheet
5.2.1 Friction of curling stone on curling rink ice
Friction of rock on curling rink ice estimated as following two methods. Average friction coefficient μ was derived from $mV_0^2/2 = \mu mgs$. Fig. 28 shows the average friction. The fiction coefficient increased in low speed region though constant for high speed. In generally, curling rock moves with weak spin. When counter clockwise spin is given, left side will decelerate in velocity therefore friction increases as shown in Fig.29. Anisotropy of friction between left and right will be cause of curl as mentioned by Harrigton (1924) and Denny (1998).

Friction coefficient as a function of velocity will be given as follows; The change of sliding distance by unit time gives velocity; the change of velocity by unit time gives μg (where, g is gravitational acceleration). Therefore if the relation between sliding distance, s, until stop and sliding time, t, could be gained, frictional coefficient μ will be given;

$$F=mdv/dt= - \mu mg$$

where F is the frictional resistance, m the mass of rock, v the velocity.

$$\mu = - (1/g)(dv/dt)= - (1/g)(d^2s/dt^2)$$

Fig. 30 shows the log-log relation between sliding distance s and time t until stop of rock.

In generally, stone is given very slow rotation (2~3 rotation until stop), it is wander the extremely low damping of angular velocity. To understand this reason, it is to clear the transverse friction component f_y and angular friction one f_θ.

Rock will almost move without decrease of angular velocity except around stop because friction to rotation becomes extremely small compare to longitudinal one.
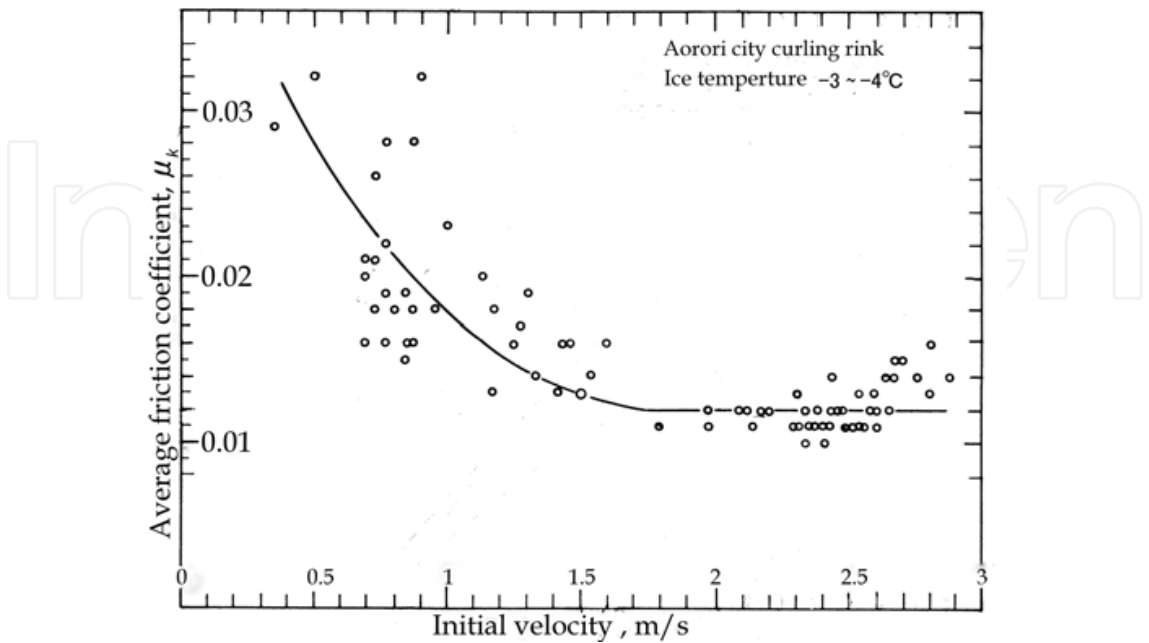

Fig. 28. Average friction coefficient of rock for initial velocity. (after Tusima, 2010)
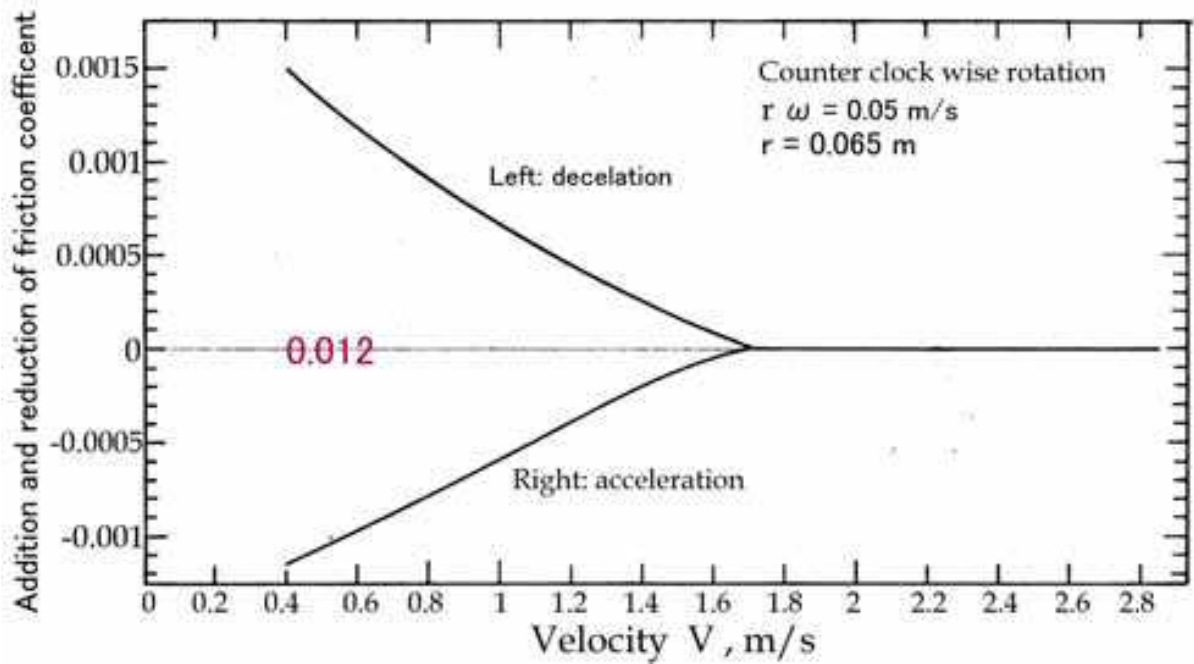
Fig. 29. Addition and reduction of friction by rotation of rock. (after Tusima, 2010)
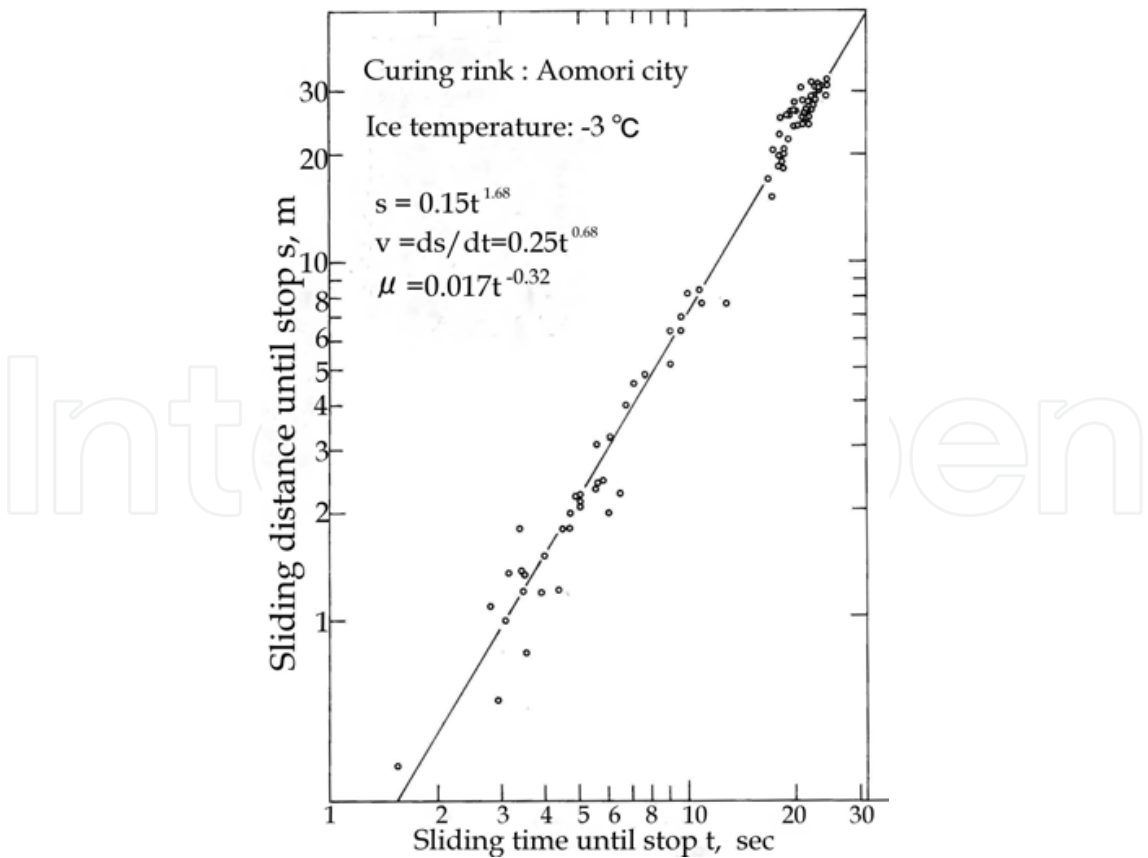

Fig. 30. Relation of sliding distance s to sliding time t until stop of rock. (after Tusima, 2010)

We suppose frictional resistance f_y as moving direction and f_θ as tangential direction of rotation. Total resistance is f. The angle between f and f_y supposed to ß.
θ is angle from x axis.

$$f_\theta = (\sin ß / \sin\theta)f$$

$$\mu_\theta = (f_\theta / f)\mu$$

$$= \{r\omega / [v^2 + 2r\omega v\cos\theta + (r\omega)^2]^{1/2}\}\mu$$

If we suppose μ of 0.01, v of 1 m/s and rω of 0.04 m/s, we will get about 0.0004 for μ_θ. This means angular velocity of rock does not almost decrease at high sliding speed.

6. Conclusion

In this chapter, it was noticed two points connected to friction: the considerably high value of ice hardness and extremely small shear strength of ice compared to hardness. This leads low friction in the view point of adhesion theory.
The friction coefficient of steel ball on flat plate of ice was low even in low speed range. The friction showed remarkable anisotropy on crystallographic plane and sliding orientation. Frictional track on ice also showed remarkable anisotropy by the crystallographic plane and sliding orientation. These frictional features were well explained by adhesion theory. The friction of speed-skate was around 0.005, and this extremely low value gave dry friction, therefore the crystallographic planes of ice reflected to the friction coefficient of skate.
In frictional research history on ice, almost research had overlooked above mechanical characteristics of ice and had thought much of fluid lubrication which based on the analogy of slipperiness and type of friction. Though the thermal analysis have explained well the frictional properties on ice, however it is not astonishing because the most frictional energy converts to heat. Thermal analysis apply to the frictional melting theory, adhesion theory and other.
In frictional melting theory, it must exist liquid water which is prepared by fusion of ice. Therefore its theory needs the heat to melt which is given by frictional heat. If the heat is insufficient (namely, extremely low friction), the theory can not apply. This is logical contradiction of frictional melting theory for slipperiness of ice. Of course, if liquid exist, it will lead to low friction by weakness of contact bond.

7. References

Ambach, W. & Mayr, B. (1981). Ski sliding and water film. *Cold Region Science and Technology*, Vol.5, pp.59-65.
Barnes, P. & Tabor, D. (1966). Plastic flow and pressure melting in deformation of ice I. *Nature*, Vol.210, pp.878-882.
Barnes, P.; Tabor, D., & Walker, J.C.F. (1971). Friction and creep of polycrystalline ice. *Proceedings of the Royal Society London*, Ser. A, Vol.324, No.1557, pp.127-155.
Bowden, F.P. (1953). Friction on snow and ice. *Proceedings of the Royal Society of London*, Ser.A, Vol.217, No.1131, pp.462-78.
Bowden, F.P. (1955). Friction on snow and ice and the development of some fast-running ski. *Nature*, Vol.176, No.4490, pp.946-47.

Bowden, F.P., & Hughes, T.P. (1939). The mechanism of sliding on ice and snow. *Proceedings of the Royal Society of London*, Ser. A, Vol.172, No.949, pp.280-98.

Bowden, F.P. & Tabor, D. (1950). T*he friction and lubrication of solids*. [Part 1.] Oxford, Clarendon Press.

Butkovich, T.R. (1954). Hardness of single ice crystals. *U.S.Snow, Ice and Permafrost Research Establishment*. Research Paper 9. 12pp.

Denny, M. (1998). Curling rock dynamics. *Can. J. Phys.* Vol.76, pp.295-304.

Evans, D.C.B.; Nye, J.F., & Cheeseman, K.J. (1976). The kinetic friction of ice. *Proceedings of the Royal Society of London*, Ser.A, Vol.347, No.1651, pp.439-512.

Furushims, T. (1972). Studies on the frictional resistance of skate. *Seppyo*, Vol.34, pp.9-14.

Harrington, L.E. (1924). An experimental study of the motion of curling stones. *Proceedings and Transactions of the Royal Society of Canada*. Vol.18, Sect. 3, pp.247-259.

Hori, T. (1956). On the supercooling and evaporation of thin water film. *Low Temperature Sience*(Hokkaido University), Ser.A, [No.] 15, pp.33-42

Huzioka, T. (1962). Studies on the resistance of snow sledge.V. T*eion-kagaku: Low Temperature Science*, Ser.A, [No.] 20, pp.159-79.

Huzioka, T. (1963). Studies on the resistance of snow sledge.Ⅵ. T*eion-kagaku: Low Temperature Science*, Ser.A, [No.]21, pp.31-44.

Itagaki, K. & Huber, N.P. (1968): Measurement of dynamic friction of ice. *Physics and chemistry of ice*. Eds. by N. Maeno & T. Hondo, pp.212-218.

Jellinek, H.H.G. (1957). Adhesive properties of ice. *SIPRE Research Report*, No.38, 20pp.

Jellinek, H.H.G. (1967). Liquid-like (transition) layer on ice. *Jounal of Colloid and Interface Science*, Vol.25, pp.192-205.

Jellinek, H.H.G. (1970). Ice adhesion and abhesion: A survey. *CRREL Special Report,* No.115, pp.46-77.

Joly, J. (1887). The phenomena of skating and Professor J.Thomson's thermodynamic relation. *Scientific Proceedings of the Royal Dublin Society*, New Series, Vol.5, Pt 6, pp.453-54.

Kobayashi, T. (1973). Studies of the properties of ice in speed skating rink. *ASHRAE Journal*, January, pp.52-56.

Koning, J.J.de; Groot, G.de, & IngenSchnau, G.J.van. (1992). Ice friction during speed skating. *J. Biomechanics*, Vol.25, pp.565-571.

Landy, M. & Freiberger, A. (1967). A studies of ice adhesion. *J. Colloid and Interface Science,* Vol.25, pp.231-244.

McConica, T.H. (1950). Sliding on ice and snow. American Ski Company, Technical Report.

Niven, C.D. (1959). A proposal mechanism for ice friction. *Canadian Journal of Physics*, Vol.37, No.3, pp.247-255.

Offenbacher, E.L. & Roselman, I.C. (1971). Hardness anisotropy of single crystal of ice Ih. *Nature, Physical Science*, Vol.234, No.49, pp.112-113.

Raraty, L.E. & Tabor, D. (1958). The adhesion and strength properties of ice. *Proceedings of the Royal Society of London*, Ser.A, Vol.245, No.1241, p.184-201.

Reynolds, O. (1899). On the slipperiness of ice. *Memoirs and Proceedings of the Manchester Literary and Philosophical Society*, Vol.43, Pt.2, No.5.

Shimbo, M., (1961). The mechanism of sliding on snow. *Union Geodesique et Geophysique Internationale. Association Internationale d'Hydrologie Scientifique.* Assemble generale

de Helsinki, 25-7-6-6 1960. Commission des Neiges et   Glaces, pp.101-06. (Publication No.54. de l'Association Internationale d'Hydrologie Scientifique.)

Tabor, D. & Walker, J.C.F. (1970). Creep and friction of ice. *Nature*, Vol.228, pp.137-139.

Tusima, K. (1976). A review of mechanism of friction of ice. *Journal of Japan Society of Lubrication Engineering*, Vol.21, pp.287-294.

Tusima, K. (1977). Friction of a steel ball on a single crystal of ice. *Journal of Glaciology*, Vol.19, No.81, pp.225-235.

Tusima, K. (1978). Anisotropy of the friction on a single crystal of ice. Journal of Glaciology, Vol.21, [No.]85, pp661-668.

Tusima, K. (2009). Tribology in skating, skiing, and curling. *Japanese Journal of Tribology,* Vol.54, [No.]7, pp.470-475.

Tusima, K. (2010). Estimation friction coefficient of stone and mechanism of curl. *Proceedings of Cold Region Technology Conference.* Vol.26, pp.422-427.

Tusima, K. & Fujii, T. (1973). Measurements of shear strength of ice. *Low Temperature Science*, Ser.A, No.31, pp.33-43.

Tusima, K., & Yosida, Z. (1969). Melting of ice by friction. *Low Temperature Science*, Ser.A, [No.]27, pp.17-30

Tusima, K.; Yuki, M., Kiuchi, T., & Shimodaira, S. (2000). Development of a high speed skating rink by the control of crystallographic plane of ice. *Japanese Journal of Tribology*, Vol.45, pp.17-26.

Weyl, W.A. (1951). Surface structure of water and some of its physical and chemical manifestation. *J. Colloid and Interface Science*, Vol.6, pp.389-405.
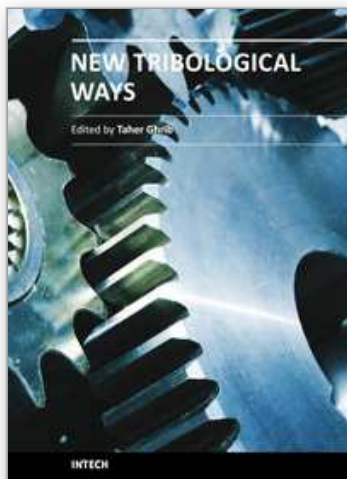
New Tribological Ways

Edited by Dr. Taher Ghrib

This book aims to recapitulate old information's available and brings new information's that are with the fashion research on an atomic and nanometric scale in various fields by introducing several mathematical models to measure some parameters characterizing metals like the hydrodynamic elasticity coefficient, hardness, lubricant viscosity, viscosity coefficient, tensile strength .... It uses new measurement techniques very developed and nondestructive. Its principal distinctions of the other books, that it brings practical manners to model and to optimize the cutting process using various parameters and different techniques, namely, using water of high-velocity stream, tool with different form and radius, the cutting temperature effect, that can be measured with sufficient accuracy not only at a research lab and also with a theoretical forecast. This book aspire to minimize and eliminate the losses resulting from surfaces friction and wear which leads to a greater machining efficiency and to a better execution, fewer breakdowns and a significant saving. A great part is devoted to lubrication, of which the goal is to find the famous techniques using solid and liquid lubricant films applied for giving super low friction coefficients and improving the lubricant properties on surfaces.

How to reference

In order to correctly reference this scholarly work, feel free to copy and paste the following:

INTECH

open science | open minds